NMC
Committed to Nuclear Excellence

Kewaunee Nuclear Power Plant
N490, State Highway 42
Kewaunee, WI 54216-9511
920-388-2560

Operated by
Nuclear Management Company, LLC

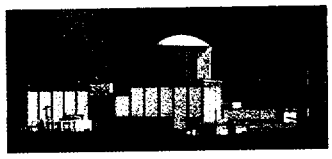

February 23, 2001

10CFR50, Appendix A, Criterion 4

U.S. NRC Nuclear Regulatory Commission
Attention: Document Control Desk
Washington, D.C. 20555

Ladies/Gentlemen:

Docket 50-305
Operating License DPR-43
Kewaunee Nuclear Power Plant
REQUEST TO EXCLUDE DYNAMIC EFFECTS ASSOCIATED WITH POSTULATED PIPE RUPTURES FROM LICENSING BASIS FOR RESIDUAL HEAT REMOVAL, ACCUMULATOR INJECTION, AND SAFETY INJECTION SYSTEM PIPING BASED UPON LEAK BEFORE BREAK ANALYSIS

In accordance with 10 CFR 50, Appendix A, General Design Criteria 4, the Nuclear Management Company, LLC, (NMC) requests Nuclear Regulatory Commission (NRC) review and approval to exclude the dynamic effects associated with postulated pipe ruptures from the Kewaunee Nuclear Power Plant (KNPP) licensing basis. This request is for portions of the KNPP Residual Heat Removal (RHR), Accumulator Injection, and Safety Injection (SI) system piping.

Specifically, the following piping at KNPP falls under the scope of this request:

1) 12-inch SI lines (Loop A and Loop B). These lines are connected to the SI accumulators. The Loop B line also serves as the RHR system return line.

2) 8-inch RHR lines (Loop A and Loop B). These lines serve as the RHR system suction lines.

3) 6-inch cold leg SI Lines (Loop A and Loop B). These lines provide flow from the high-pressure SI pumps.

4) 6-inch reactor vessel SI lines (Loop A and Loop B). These lines are composed of 4-inch diameter lines for some distance from the reactor vessel nozzle and a shorter section of 6-inch diameter line near the isolation valves. Although these lines are included in the evaluation, the maximum break flow would be limited by the 4-inch piping.

The attached analyses demonstrate that the probability of fluid system piping rupture is extremely low under conditions consistent with the design basis for this piping. These analyses are based upon guidance from NUREG-1061, Volume 3 and Standard Review Plan Section

A001

3.6.3. Furthermore, additional analysis has been performed to address the application of leak-before-break (LBB) to small diameter piping consistent with guidance from NUREG/CR-6443 and NUREG/CR-4572. Finally, it should be noted that this application is acceptable for these analyzed portions of piping since a minimum detectable leak rate of 0.25 gallons per minute has been conservatively used for the LBB evaluation for KNPP.

NMC requests the approval of this analysis by December 31, 2001.

Please contact Mr. Tom Webb at 920-388-8537 or Mr. Charles Tomes at (920-433-1729 if there are any questions or if we can be of assistance regarding the review of this request.

Sincerely,

Mark E. Reddemann
Site Vice President

CAT

Attach.

cc - US NRC – Region III
NRC Senior Resident Inspector
Electric Division, PSCW

ATTACHMENT 1

Letter from M. E. Reddemann (NMC)

To

Document Control Desk (NRC)

Dated

February 23, 2001

Structural Integrity Technical Report

Structural Integrity Associates, Inc.

www.structint.com

Report No.: SIR-00-045
Revision No.: 0
Project No.: WPS-02Q
File No.: WPS-02Q-401
October 2000

Leak-Before-Break Evaluation
6-inch to 12-inch Safety Injection and Residual Heat Removal Piping Attached to the RCS
Kewaunee Nuclear Power Plant

Prepared for:

Wisconsin Public Service
Contract No. 255443

Prepared by:

Structural Integrity Associates, Inc.
San Jose, California

Prepared by: _____ Date: 10/4/2000
N. G. Cofie, Ph.D.

Reviewed and Approved by: _____ Date: 10/4/2000
A. F. Deardorff, P.E.

REVISION CONTROL SHEET

Document Number: SIR-00-045

Title: Leak-Before-Break Evaluation, 6-inch to 12-inch Safety Injection and Residual Heat Removal Piping Attached to the RCS Kewaunee Nuclear Power Plant

Client: Wisconsin Public Service

SI Project Number: WPS-02Q

Section	Pages	Revision	Date	Comments
-	i – x	0	10/4/00	Initial Issue
1	1-1 – 1-9			
2	2-1 – 2-2			
3	3-1 – 3-3			
4	4-1 – 4-12			
5	5-1 – 5-42			
6	6-1 – 6-16			
7	7-1 – 7-2			
8	8-1 – 8-3			
App. A	A-0 – A-4			

SUMMARY

This report presents a leak-before-break (LBB) evaluation for piping systems attached to the reactor coolant system (RCS) at Kewaunee Nuclear Power Plant (operated by Wisconsin Public Service Corporation). The evaluation includes portions of the safety injection (SI) and residual heat removal (RHR) systems. It was performed jointly with the Prairie Island Nuclear Generating Plant, Units 1 and 2 (operated by Northern States Power Company) to take advantage of the similarities of these plants in the LBB evaluations. As such, some of the evaluation results presented in this report are generic to all three units.

The LBB evaluation was performed in accordance with the 10 CFR 50, Appendix A GDC-4 and NUREG-1061, Vol. 3 as supplemented by NUREG-0800, Standard Review Plan 3.6.3. Additional criteria to address the application of LBB to small diameter piping taking guidance from NUREG/CR-6443 and NUREG/CR-4572 was developed in Section 5 of this report.

The evaluation is based on determining critical flaw sizes and leakage rates at all weld locations using weld-specific loads. The critical flaw size as used herein refers to the flaw length which becomes unstable under a given set of applied loads. Critical flaw sizes were calculated using both the net section plastic collapse and the elastic-plastic fracture mechanics (EPFM) J-Integral/Tearing Modulus (J/T) approach with conservative generic material properties. The "leakage flaw size" was determined as the minimum of one half the critical flaw size with a factor of unity on normal operating plus SSE loads or the critical flaw size with a factor of $\sqrt{2}$ on normal operating plus SSE loads. Thus, the leakage flaw size as referred herein maintains a safety factor of 2 on the critical flaw size under normal plus SSE loads and a safety factor of 1 when the loads are factored by $\sqrt{2}$. Leakage rates were then calculated through the leakage flaw sizes per the requirements of NUREG-1061. The determination of critical flaw sizes and leak rates took into account the effects of restraint of pressure induced bending which has been shown to affect LBB analysis results especially for small diameter piping. A fatigue crack growth analysis was also performed to determine the growth of postulated semi-elliptical, inside surface flaws with an initial size based on ASME Code Section XI acceptance standards.

The following summary of the LBB evaluation is formatted along the lines of the "Recommendations for Application of the LBB Approach" in the NUREG-1061 Vol. 3 executive summary:

(a) The SI and RHR piping systems are constructed of very ductile stainless steel that is not susceptible to cleavage-type fracture. In addition, it has been shown that these systems are not susceptible to the effects of corrosion, high cycle fatigue or water hammer.

(b) Loadings have been determined from the original piping analysis, and are based upon pressure, dead weight, thermal expansion and earthquake seismic motion. All highly-stressed locations in the piping were considered.

(c) Although plant specific certified material test report (CMTR) data is available, this information alone is not complete for the fracture mechanics evaluations. As such, lower-bound generic industry material properties for the piping and welds have been conservatively used in the evaluations.

(d) Crack growth analysis was conducted at the most critical locations on all the evaluated piping, considering the cyclic stresses predicted to occur over the life of the plant. For a hypothetical flaw with aspect ratio of 10:1 and an initial flaw depth of approximately 11% of pipe wall, it will take about 38 heatup and cooldown cycles to grow the hypothetical flaw to the ASME Section XI allowable flaw size (75% of pipe wall) at the most critical location. For the last ten years, Kewaunee has experienced 13 heatup/cooldown cycles. Given that this piping is inspected in accordance with ASME Section XI requirements in each 10-year interval, it is believed that crack growth can be managed by the current in-service inspection program.

(e) Based on evaluation of the critical cracks at all locations in the piping system, it was determined that the leakage at the limiting location was 3.74 gpm. With a margin of 10 on leakage suggested in NUREG-1061 Vol. 3, the leakage detection system at Kewaunee

is capable of measuring leakage of 2.5 gpm. This leakage detection is assumed in the LBB evaluation.

(f) Since the systems considered in this evaluation consist of relatively small diameter piping (6-inch to 12-inch OD), the effect of the piping system flexibility and restraint was considered in the determination of the critical flaw sizes and leakage rates at the various weld locations. The most highly restrained piping systems were analytically modeled and various crack configurations were introduced at the weld locations to determine the reduction in applied moments due to piping system restraint. The leakage was then calculated. This evaluation showed that there was not a significant reduction in leakage as a result of piping system restraint.

(g) Crack growth of a leakage size crack in the length direction due to an SSE event is no more than 1% of the leakage flaw size. This is not significant compared to the margin between the leakage-size crack size and the critical crack size.

(h) For all locations, the critical size circumferential crack was determined for the combination of normal plus safe shutdown earthquake (SSE) loads. The leakage size crack was chosen such that its length was no greater than the critical crack size reduced by a factor of two. Axial cracks were not considered since critical axial cracks always exhibit much higher leakage and more margin than critical circumferentially-oriented cracks.

(i) For all locations, the critical crack size was determined for the combination of $\sqrt{2}$ times the normal plus SSE loads. The leakage size crack was selected to be no greater than this critical crack size. (The minimum of the crack sizes determined by this criterion, and that of the criterion of (h) above, was chosen for calculation of the leakage rate for each location.)

(j-n) No special testing (other than information in the CMTRs) was conducted to determine material properties for fracture mechanics evaluation. Instead, generic lower bound

material toughness and tensile properties were used in the evaluations. The material properties so determined have been shown to be applicable near the upper range of normal plant operation and exhibit ductile behavior at these temperatures. This data is widely accepted by industry for conducting mechanics analysis.

(o) Limit load analysis as outlined in NUREG-0800, SRP 3.6.3, was utilized in this evaluation to supplement the EPFM J/T analyses in order to determine the critical flaw sizes. The most limiting results of these two analytical approaches were used in determining the critical flaw sizes for the various piping systems.

Thus, it is concluded that the 6-inch to 12-inch piping evaluated in this report qualifies for the application of leak-before-break analysis to demonstrate that it is very unlikely that the piping could experience a large pipe break prior to leakage detection.

Table of Contents

List of Tables

List of Tables
(Continued)

List of Figures

1.0 INTRODUCTION

1.1 Background

This report documents evaluations performed by Structural Integrity Associates (SI) to determine the leak-before-break (LBB) capabilities of the high energy non-isolable 6-inch to 12-inch piping attached to the reactor coolant system (RCS) at Kewaunee Nuclear Power Plant. These encompass portions of the safety injection (SI) system, including that from the SI accumulators, and the residual heat removal (RHR) piping. These evaluations were undertaken to address the potential for high energy line break at these locations. The portions of these lines evaluated extend from the nozzle at the reactor coolant loop to the first isolation valve.

The evaluations were performed jointly with Prairie Island Units 1 and 2 since the plants are very similar, therefore allowing some portions of the evaluation to be performed generically for all three units. Specific results of the LBB evaluation for Prairie Island Units 1 and 2 are provided in Reference 1. It should be noted that all the piping included in the evaluation as delineated below are also present at Prairie Island Units 1 and 2. However, in addition to these lines, Prairie Island also has a 6-inch RCS draindown line on the hot leg (Loop A on Unit 1 and Loop B on Unit 2). This line at Prairie Island was added to the plant following initial construction and consists of a short section of 6-inch diameter piping prior to reducing to 2-inch diameter at the isolation valve. The draindown line is not present at Kewaunee; hence reference to the draindown lines in this report is made only as part of the generic evaluation and does not specifically apply to Kewaunee.

The following lines are evaluated in this report:

- 12-inch SI lines (Loop A and Loop B). These lines are connected to the SI accumulators. The Loop B line also serves as the RHR system return line.
- 8-inch RHR lines (Loop A and Loop B). These lines serve as the RHR system suction lines.
- 6-inch cold leg SI lines (Loops A and B). These lines provide flow from the high pressure SI pumps.
- 6-inch capped nozzles on the hot leg (Loops A and B).

In addition to the above lines, there are also SI lines connected to the reactor vessel (Loops A and B). These lines are composed of 4-inch diameter lines for some distance from the reactor vessel nozzle and a shorter section of 6-inch diameter line near the isolation valves. For these lines, the maximum break flow would be limited by the 4-inch piping and hence these lines were not evaluated.

1.2 Leak-Before-Break Methodology

NRC SECY-87-213 [2] covers a rule to modify General Design Criterion 4 (GDC-4) of Appendix A, 10 CFR Part 50. This amendment to GDC-4 allows exclusion from the design basis of all dynamic effects associated with high energy pipe rupture by application of LBB technology.

Definition of the LBB approach and criteria for its use are provided in NUREG-1061 [3], supplemented by NUREG-0800, SRP 3.6.3 [4]. Volume 3 of NUREG-1061 defines LBB as "...the application of fracture mechanics technology to demonstrate that high energy fluid piping is very unlikely to experience double-ended ruptures or their equivalent as longitudinal or diagonal splits." The particular crack types of interest include circumferential through-wall cracks (TWC) and part-through-wall cracks (PTWC), as well as axial or longitudinal through-wall cracks (TWC), as shown in Figure 1-1.

LBB is based on a combination of in-service inspection (ISI) and leak detection to detect cracks, coupled with fracture mechanics analysis to show that pipe rupture will not occur for cracks smaller than those detectable by these methods. A discussion of the criteria for application of LBB is presented in Section 2 of this report, which summarizes NUREG-1061, Vol. 3 requirements.

The approach to LBB which has gained acceptance for demonstrating protection against high energy line break (HELB) in safety-related nuclear piping systems is schematically illustrated in Figure 1-2. Essential elements of this technique include critical flaw size evaluation, crack propagation analysis, volumetric nondestructive examination (NDE) for flaw detection/sizing, leak detection, and service experience. In Figure 1-2, a limiting circumferential crack is modeled as

having both a short through-wall component, or an axisymmetric part-through-wall crack component. Leak detection establishes an upper bound for the through-wall crack component while volumetric ISI limits the size of undetected part-through-wall defects. These detection methods complement each other, since volumetric NDE techniques are well suited to the detection of long cracks while leakage monitoring is effective in detecting short through-wall cracks. The level of NDE required to support LBB involves volumetric inspection at intervals determined by fracture mechanics crack growth analysis, which would preclude the growth of detectable part-through-wall cracks to a critical size during an inspection interval. A fatigue evaluation is performed to ensure that an undetected flaw acceptable per ASME Section will not grow significantly during service. For through-wall defects, crack opening areas and resultant leak rates are compared with leak detection limits.

The net effect of complementary leak detection and ISI is illustrated by the shaded region of Figure 1-2 as the largest undetected defect that can exist in the piping at any given time. Critical flaw size evaluation, based on elastic-plastic fracture mechanics techniques, is used to determine the length and depth of defects that would be predicted to cause pipe rupture under specific design basis loading conditions, including abnormal conditions such as a seismic event and including appropriate safety margins for each loading condition. Crack propagation analysis is used to determine the time interval in which the largest undetected crack could grow to a size which would impact plant safety margins. A summary of the elements for a leak-before-break analysis is shown in Figure 1-3. Service experience, where available, is useful to confirm analytical predictions as well as to verify that such cracking tends to develop into "leak" as opposed to "break" geometries.

In accordance with NUREG-1061, Vol. 3 [3] and NUREG-0800, SRP 3.6.3 [4], the leak-before-break technique for the high energy piping systems evaluated in this report included the following considerations.

- Elastic-plastic fracture mechanics analysis of load carrying capacity of cracked pipes under worst case normal loading, with safe-shutdown earthquake (SSE) loads included. Such analysis includes elastic-plastic fracture data applicable to pipe weldments and weld heat affected zones where appropriate.

- Limit-load analysis in lieu of the elastic-plastic fracture mechanics analysis described above.

- Linear elastic fracture mechanics analysis of subcritical crack propagation to determine ISI (in-service inspection) intervals for long, part-through-wall cracks.

- A piping system evaluation to determine the effect of piping restraint on leakage for small diameter piping.

Piping stresses have a dual role in LBB evaluations. On one hand, higher maximum (design basis) stresses tend to yield lower critical flaw sizes, which result in smaller flaw sizes for assessing leakage. On the other hand, higher operating stresses tend to open cracks more for a given crack size and create a higher leakage rate. Because of this duality, the use of a single maximum stress location for a piping system may result in a non-conservative LBB evaluation. Thus, the LBB evaluation reported herein has been performed for each nodal location addressed in the plant piping system analysis.

1.3 Leak Detection Capability at Kewaunee

Application of LBB evaluation methodology is predicated on having a very reliable leak detection system at the plant, capable of measuring 1/10 of the leakage determined in the evaluation. Section 6.5 of Kewaunee FSAR [5] provides details of the capabilities of the leak detection systems. Several leak detection systems are employed for the reactor coolant system but the four most important ones are described below.

Containment System Air Particulate Monitor (R-11)

This is the most sensitive instrument available for detection of Reactor Coolant System (RCS) leakage in containment. It is capable of detecting low levels of radioactivity in containment air. Assuming complete dispersion of leaking radioactive solids consistent with very little or no fuel cladding leakage, R-11 is capable of detecting leaks as small as approximately 0.013 gpm (50

cm^3/min) within 20 minutes. Even if only 10% of the particulate activity is actually dispersed, leakage rate of the order of 0.13 gpm are well within detectable range of R-11.

Containment Radiogas Monitor (R-12)

The containment radioactive gas monitor is inherently less sensitive (threshold at 10E-6 μCi/cc) than the containment air particulate monitor, and would function in the event that significant reactor coolant gaseous activity exists from fuel cladding defects. Assuming a reactor coolant activity of 0.3 μCi/cc, the occurrence of a leak of 2 to 4 gpm would double the zero leakage background in less than an hour's time. In these circumstances this instrument is a useful backup to the air particulate monitor.

Humidity Detection

The humidity detection instrumentation offers another means of detection of leakage into the containment. Although this instrumentation is not as sensitive as the air particulate monitor, it has the characteristics of being sensitive to vapor originating from all sources within the containment, including the Reactor Coolant, Steam and Feedwater Systems. Plots of containment air dew point variations above a base-line maximum established by the cooling water temperature to the air coolers should be sensitive to incremental leakage equivalent to 2 to 10 gpm.

Containment Sump Leakage Measuring

This leak detection method is based on the principle that the leakage collected by the containment sump will be pumped to the waste holdup tank, with pumping time directly related to the quantity of leakage. Sump pump running time is monitored in the control room, and will provide an indication of deviation from normal leakage rates to the operator.

Since the fan-coil units drain to the Containment Vessel sump (Sump A), all condensation from primary coolant leaks is directed to the containment sump. Detection of leakage is possible within 30 to 40 minutes. Leak rates of approximately 0.5 gpm are detectable by this method. Larger leakage rates are detectable in much shorter time periods.

In summary, Kewaunee has a very redundant leak detection system capable of detecting leakage as low as 0.013 gpm. However, based on the similarity of Kewaunee and R. E. Ginna Nuclear Power plants and the fact that a leak detection of 0.25 gpm was approved by the NRC for use at Ginna [6], a minimum detectable leakage rate of 0.25 gpm has been conservatively used for the LBB evaluation for Kewaunee. Since NUREG-1061, Vol. 3 requires that a margin of 10 be provided on leakage, the minimum allowable evaluated leakage rate is 2.5 gpm.

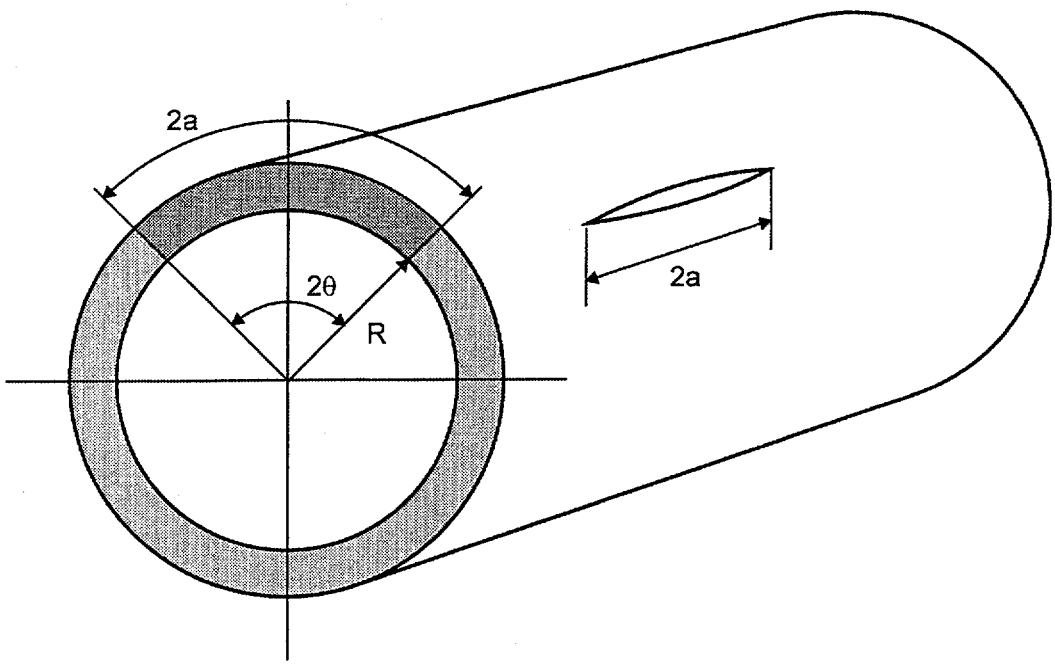

a. Circumferential and Longitudinal Through-Wall Cracks of Length 2a.

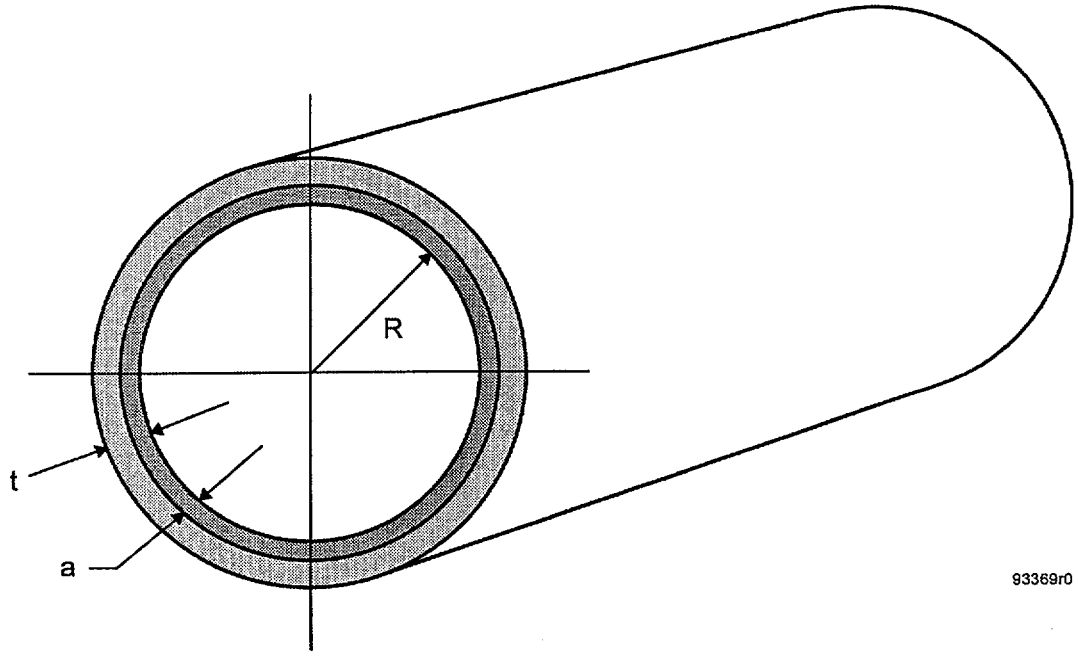

b. Circumferential 360 Part-Through-Wall Crack of Depth a.

Figure 1-1. Representation of Postulated Cracks in Pipes for Fracture Mechanics Leak-Before-Break Analysis

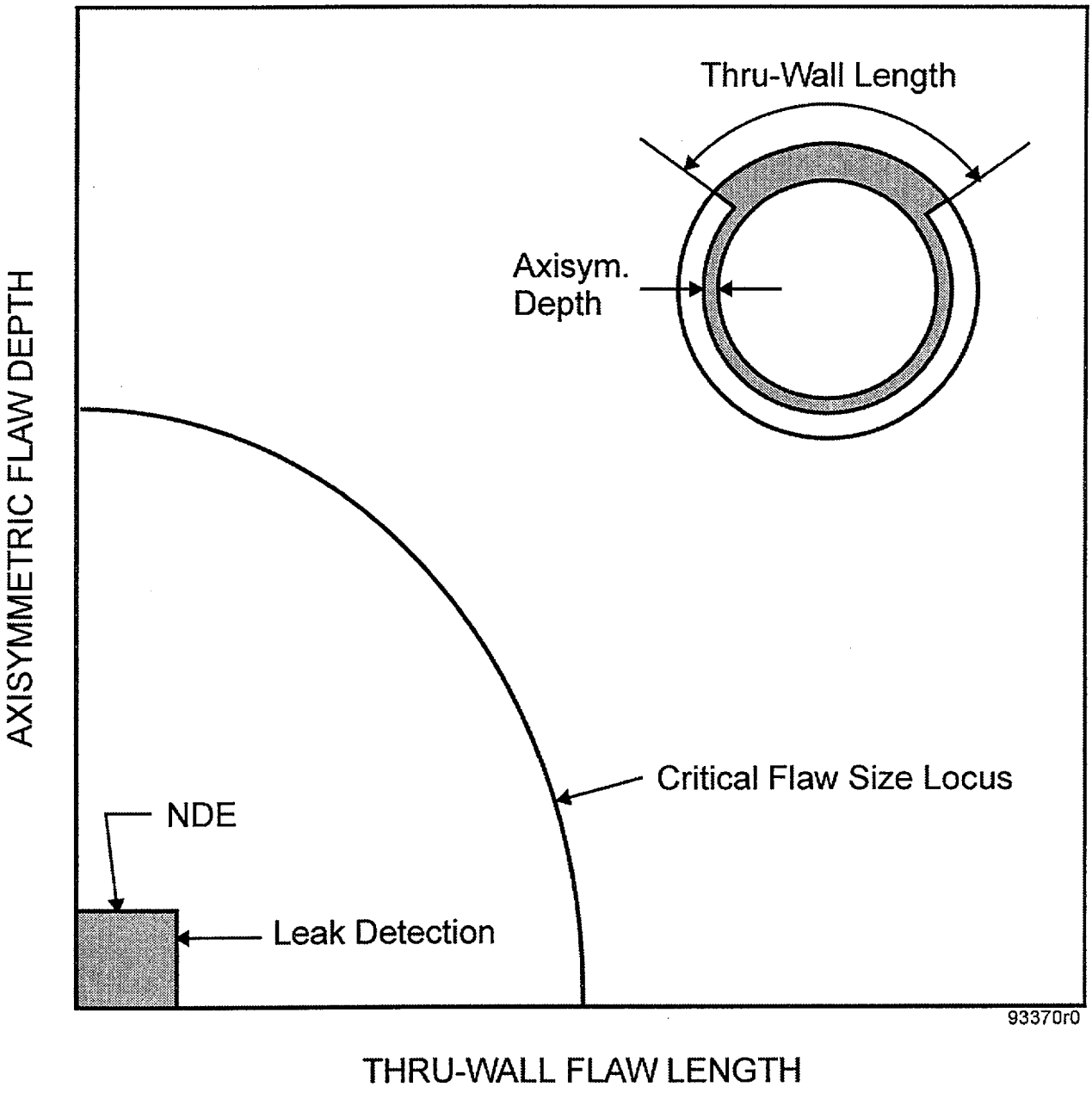

Figure 1-2. Conceptual Illustration of ISI (UT)/Leak Detection Approach to Protection Against Pipe Rupture

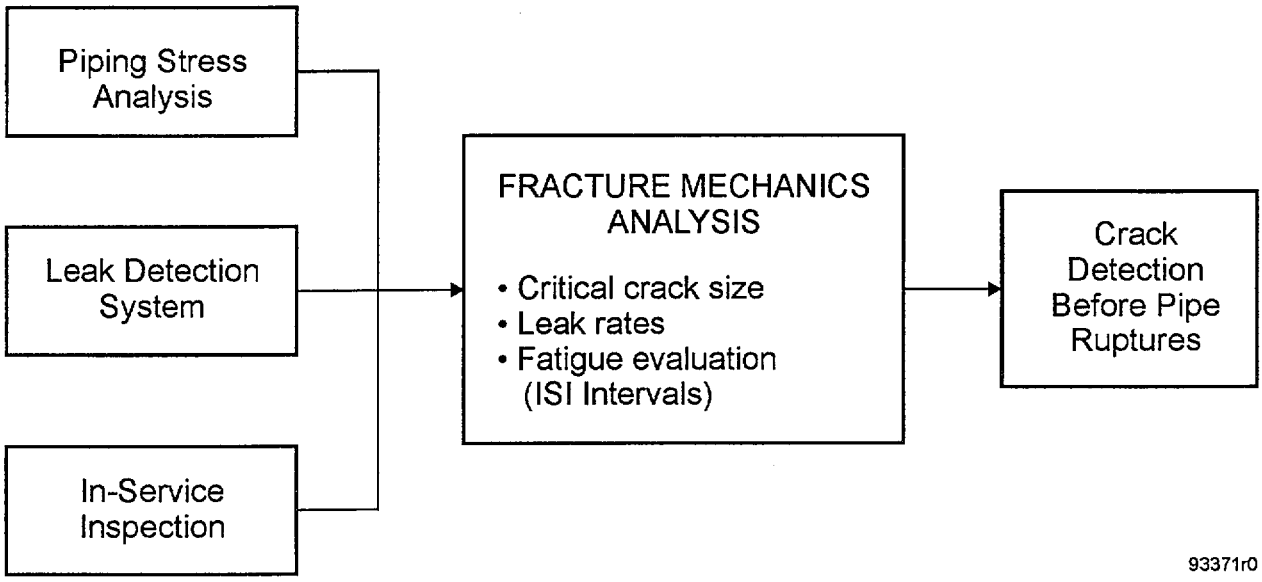

Figure 1-3. Leak-Before-Break Approach Based on Fracture Mechanics Analysis with In-service Inspection and Leak Detection

2.0 CRITERIA FOR APPLICATION OF LEAK-BEFORE-BREAK

NUREG-1061, Vol. 3 [3] identifies several criteria to be considered in determining applicability of the leak-before-break approach to piping systems. Section 5.2 of NUREG-1061, Vol. 3 provides extensive discussions of the criteria for performing leak-before-break analyses. These requirements are restated in NUREG-0800, SRP 3.6.3 [4]. The details of the discussions are not repeated here; the following summarizes the key elements:

2.1 Criteria for Through-Wall Flaws

Acceptance criteria for critical flaws may be stated as follows:

1. A critical flaw size shall be determined for normal operating conditions plus safe shutdown earthquake (SSE) loads. Leakage for normal operating conditions must be detectable for this flaw size reduced by a factor of two.

2. A critical flaw size shall be determined for normal operating conditions plus SSE loads multiplied by a factor of $\sqrt{2}$. Leakage for normal operating conditions must be detectable for this flaw size.

It has been found in previous evaluations conducted by Structural Integrity Associates (SI) that in general, the first criterion bounds the second. However, in this evaluation, both criteria were considered for completeness.

Either elastic-plastic fracture mechanics instability analysis or limit load analysis may be used in determining critical flaw sizes. NUREG-0800 SRP 3.6.3 [4] provides a modified limit load procedure that may be used for austenitic piping and weldments. Both approaches have been used in this evaluation as presented in Section 5.0 of the report.

2.2 Criteria for Part-Through-Wall Flaws

NUREG-1061, Vol. 3 [3] requires demonstration that a long part-through-wall flaw which is detectable by ultrasonic means will not grow due to fatigue to a depth which would produce instability over the life of the plant. This is demonstrated in Section 6.0 of this report, where the analysis of subcritical crack growth is discussed.

2.3 Consideration of Piping Restraint Effects

It was shown in References 21 that restraint of pressure induced bending in a piping system could affect the LBB analysis results. This has been shown to be especially important for small diameter piping (less than 10 inch NPS). An evaluation was therefore performed in Section 5.3 to address this issue for the small diameter piping at Kewaunee.

2.4 Consideration of Other Mechanisms

NUREG-1061, Vol. 3 [3] limits applicability of the leak-before-break approach to those locations where degradation or failure by mechanisms such as water hammer, erosion/corrosion, fatigue, and intergranular stress corrosion cracking (IGSCC) is not a significant possibility. These mechanisms were considered for the affected piping systems, as reported in Section 3 of this report.

3.0 CONSIDERATION OF WATER HAMMER, CORROSION AND FATIGUE

NUREG-1061, Vol. 3 [3] states that LBB should not be applied to high energy lines susceptible to failure from the effects of water hammer, corrosion or fatigue. These potential failure mechanisms are thus discussed below with regard to the affected RCS attached RHR and SI piping at Kewaunee, and it is concluded that the above failure mechanisms do not invalidate the use of LBB for this piping system.

3.1 Water Hammer

A comprehensive study performed in NUREG-0927 [7] indicated that the probability of water hammer occurrence in the residual heat removal systems of a PWR is very low. In NUREG-0927, only a single event of water hammer was reported for PWR residual heat removal systems with the cause being incorrect valve alignment. There was no indication as to which portion of the system was affected but it would not be that portion adjacent to the RCS-attached piping evaluated for LBB.

It was also reported in NUREG-0927 that the safety significance of water hammer events in the safety injection system is moderate. With four water hammer events reported in the SI systems, three of these events were associated with voided lines and the other event was associated with steam bubble collapse. Although there was no indication of the affected portions of the SI system, the portions susceptible to water hammer would not be that adjacent to the RCS-attached piping evaluated for LBB.

The portions of the piping evaluated for LBB are inboard of the first isolation valves for the SI and RHR piping. Thus, during normal operation, these lines experience reactor coolant pressure and temperature conditions such that there is no potential for steam/water mixtures that might lead to water hammer. The portions of these systems that are adjacent to the reactor coolant piping are not in use during normal operation. The RHR system is not used except during low-pressure low-temperature cooldown conditions. The SI system is used only during loss of coolant-accident (LOCA) conditions. During normal plant operation, the portions of the system beyond the first

isolation valve are expected to run at low temperature conditions. Thus, there should never be any voiding or potential for steam bubble collapse, which could result in water hammer loads on the piping attached directly to the RCS considered in this evaluation. To date, there has been no experience related to water hammer events in either the RHR or SI systems at Kewaunee.

As such, this phenomenon will have no impact on the LBB analysis for the affected portions of the safety injection and residual heat removal systems at Kewaunee.

3.2 Corrosion

Two corrosion damage mechanisms which can lead to rapid piping failure are intergranular stress corrosion cracking (IGSCC) in austenitic stainless steel pipes and flow-assisted corrosion (FAC) in carbon steel pipes. IGSCC has principally been an issue in austenitic stainless steel piping in boiling water reactors [8] resulting from a combination of tensile stresses, susceptible material and oxygenated environment. IGSCC is not typically a problem for the primary loop of a PWR such as the SI and RHR systems under consideration since the environment has relatively low concentrations of oxygen.

FAC is not anticipated to be a problem for this system since it is fabricated from stainless steel piping which is not susceptible to FAC.

3.3 Fatigue

Metal fatigue in piping systems connected to the reactor coolant loops of Westinghouse-designed pressurized water reactor was identified in Bulletin 88-08 [9]. Evaluations performed by Wisconsin Public Service Corporation and submitted to the Nuclear Regulatory Commission have concluded that this does not apply to Kewaunee. For the SI piping, there is no interconnection to the charging pumps that will lead to inleakage leading to cracking such was identified at Farley and Thihange. For the RHR piping, any outleakage at the isolation valve leak off lines is monitored and can be corrected such that cracking similar to that identified at the Japanese Genkai plant will not occur. Thus, there is no potential for unidentified high cycle fatigue.

Known fatigue loadings and the resultant possible crack growth have been considered by the analyses reported in Section 6.0 of this report. Based on the results presented in Section 6.0, it is concluded that fatigue will not be a significant issue for the SI and RHR piping at Kewaunee.

4.0 PIPING MATERIALS AND STRESSES

4.1 Piping System Description

The piping systems considered in this evaluation have been described in Section 1.1. Schematics of the mathematical models for these lines including selected nodal points are shown in Figures 4-1 through 4-3. The lines are fabricated from Schedule 140 and 160 stainless steel piping. From Reference 10, the RCS operating pressure is 2235 psig while the operating temperature for the cold leg is 550°F. Because of the similarities of Kewaunee and Prairie Island Units 1 and 2, the hot leg temperature was assumed to be 607.4°F, the maximum hot leg temperature reported for Prairie Island Units 1 and 2 [1].

Wisconsin Public Service Corporation plans to replace the existing Model 51 steam generators at Kewaunee with Model 54F generators in the Fall of 2001. The new operating temperatures after the replacement are listed in Table 4-1 [11]. It can be seen that in all cases, the hot leg temperature (T_{hot}) and the cold leg temperature (T_{cold}) are bounded by the temperatures used in the LBB evaluations (607.4°F and 550°F, respectively). Hence, from an operating temperature viewpoint, the LBB evaluation performed herein bounds the conditions after the replacement.

4.2 Material Properties

The material properties of interest for fracture mechanics and leakage calculations are the Modulus of Elasticity (E), the yield stress (S_y), the ultimate stress (S_u), the Ramberg-Osgood parameters for describing the stress strain curve (α and n), the fracture toughness (J_{IC}) and power law coefficient for describing the material J Resistance curve (C and N).

NUREG-1061, Vol. 3 requires that actual plant specific material properties including stress-strain curves and J-R material properties be used in the LBB evaluations. In lieu of this requirement, material properties associated with the least favorable material and welding processes from industry wide generic material sources have been used to provide a conservative assessment of critical flaw sizes and leakage rates.

The piping material is A-376, Type 316 stainless steel [10]. The piping was fabricated using gas tungsten arc welding (GTAW) process for the root, and filled using the shielded metal arc welding (SMAW) process. The worst properties of GTAW and SMAW weldments have been used in the evaluation. Several studies have shown that of these three materials, the SMAW weldment, because of its low toughness and susceptibility to thermal aging, has the most conservative properties for estimation of critical flaw sizes. Hence, properties of SMAW have been conservatively used in this evaluation. The conservative stress-strain properties for the SMAW weldments at 550°F in Reference 13, which formed the basis for the flaw acceptance criteria in ASME Section XI, were used for the evaluation. However, for the J-R curve properties, the values provided in Reference 13 for SMAW weldments were compared with the lower bound curve provided in NUREG-6428 [14] for thermally aged welds at 550°F. It was found that the lower bound curve in NUREG-6428 is more conservative and therefore was used in this evaluation. The material properties at the hot leg temperature of 607.4°F were determined by adjusting the properties at 550°F by the ratio of the values in ASME Code Section III. The Ramberg-Osgood parameters were determined at 650°F as presented in Appendix A of this report and the values at 607.4°F were then interpolated from the values at 550°F and 650°F. The fracture toughness is not expected to change significantly from 550°F to 607.4°F and therefore the J-R curve from Reference 14 was also assumed at 607.4°F. The properties used for the SMAW weldments are shown in Table 4-2.

4.3 Piping Moments and Stresses

The piping moments and stresses considered in the LBB evaluation are due to pressure (P), dead weight (DW), thermal expansion (TE) and safe shutdown earthquake inertia (SSE) consistent with the guidance provided in NUREG-1061, Vol. 3. Per the guidance provided in NUREG-1061, other secondary stresses such as residual stresses and through-wall thermal stresses were not included in the evaluation.

Piping analysis was provided in Reference 10 and included moments for the nozzles, elbows and pipe-to-valve welds for all components. Summaries of the piping moments are shown in Tables

4-3 through 4-5, respectively. For calculation of critical flaw size, the moment and stress combination of pressure, dead weight, thermal expansion and SSE loads is used with a factor of unity and factor of $\sqrt{2}$. For leakage calculations, the moment and stress combination of pressure, deadweight and thermal expansion loads is used. These basic moment load combinations are shown in Tables 4-3 through 4-5 for the various nodal locations. Stresses were calculated directly from the piping analysis moments for the various lines considered in this evaluation [10]. The resulting stresses used in the fracture mechanics analysis do not include the effects of stress indices.

The axial stress due to normal operating pressure is calculated from the expression:

$$\sigma_p = \frac{pD_i^2}{D_o^2 - D_i^2}$$

where p is the internal pressure, D_o is the outside diameter of the pipe and D_i is the inside diameter.

The bending stress due to dead weight, thermal expansion and SSE is calculated from the bending moments using the expression:

$$\sigma_m = \frac{\sqrt{M_x^2 + M_y^2 + M_z^2}}{Z}$$

where: Z = the section modulus and,

M_x, M_y, M_z = the three orthogonal moments.

Axial loads due to dead weight, thermal expansion, and seismic were not available from the piping stress analysis and therefore were not considered in the evaluation. The stresses due to axial loads are not significant compared to those from pressure loads, so their exclusion does not significantly affect the results of this evaluation.

Table 4-1

RCS Operating Temperature for Kewaunee After Replacement with Model 54F Steam Generators

Temperature Description (°F)	Case			
	1[1]	2[2]	3[3]	4[4]
T_{Hot}	586.3	586.3	606.8	606.8
T_{Cold}	521.9	521.9	543.8	543.8
$T_{Average}$	554.4	554.4	575.3	575.3
$T_{SG\ Outlet}$	521.7	521.7	543.6	543.6
$T_{Core\ Outlet}$	590.8	590.8	611.0	611.0
$T_{Average\ (zero\ load)}$	547	547	547	547

Notes:

(1) New normal operating temperature
(2) Same as Case 1 with 10% of tubes plugged
(3) Same as Case 1 except $T_{Average} = 575.3°F$
(4) Same as Case 2 except $T_{Average} = 575.3°F$

Table 4-2

Lower Bound SMAW Material Properties Used in the LBB Evaluation [13, 14]

Parameter	Value	
Temp (°F)	550 (Cold Leg)	607.4 (Hot Leg)
E (ksi)	25×10^3	24.72×10^3
$S_y = \sigma_O$ (ksi)	49.4	48.137
S_u (ksi)	61.4	61.4
$S_f = 0.5 (S_y + S_u)$ (ksi)	55.4	54.77
Ramberg-Osgood Parameter α	9.0	9.130
Ramberg-Osgood Parameter n	9.8	9.636
J_{IC} (in-k/in^2)	0.288	0.288
J-R Curve Parameter C_1 (in-k/in^2)	3.816	3.816
J-R Curve Parameter N	0.643	0.643
J_{max} (in-k/in^2)	2.345	2.345

Table 4-3

Moments for the 6-inch Safety Injection Piping Attached to Cold Leg

Nodes	DW + TE				DW + TE + SSE			
	Moment, ft-lbs				Moment, ft-lbs			
	M_x	M_y	M_z	SRSS[(1)]	M_x	M_y	M_z	SRSS[(1)]
275a	536	54	1032	1164	700	98	1378	1549
275b	332	202	1289	1346	534	306	1713	1820
277	332	202	1289	1346	534	306	1713	1820
280	232	252	1336	1379	436	382	1758	1851
560a	-752	-124	-729	1055	-816	-152	-811	1160
560b	-553	-34	-922	1076	-649	-76	-1022	1213
563	-553	-34	-922	1076	-649	-76	-1022	1213
565	-455	-4	-967	1069	-559	-50	-1067	1206

(1) $\text{SRSS} = \sqrt{M_x^2 + M_y^2 + M_z^2}$

Table 4-4

Moments for the 12-inch Safety Injection Piping Attached to Cold Leg

Nodes	DW + TE				DW + TE + SSE			
	Moment, ft-lbs				Moment, ft-lbs			
	M_x	M_y	M_z	SRSS[(1)]	M_x	M_y	M_z	SRSS[(1)]
110	-30844	11183	-50110	59895	-31422	12893	-51140	61391
112	-25922	17896	-58699	66617	-26436	19764	-59499	68041
115	-18949	27207	-70874	78246	-19427	29713	-71370	79712
119	-17883	28595	-72736	80175	-18363	31231	-73190	81666
120a	-17884	28593	-72733	80172	-18364	31229	-73187	81663
120b	-5501	36923	-77583	86097	-6917	40411	-77801	87943
125	-5501	36923	-77583	86097	-6917	40411	-77801	87943
310	52212	-28479	31924	67500	52874	-29519	32636	68791
315a	52216	-28482	31924	67505	52878	-29522	32636	68795
315b	61105	-37049	21756	74698	61971	-38065	22498	76128
320	61105	-37049	21756	74698	61971	-38065	22498	76128
330	59193	-37049	19179	72417	60347	-38065	19957	74088

(1) $SRSS = \sqrt{M_x^2 + M_y^2 + M_z^2}$

Table 4-5

Moment for the 8-inch Residual Heat Removal Piping Attached to Hot Leg

Nodes	DW + TE				DW + TE + SSE			
	Moment, ft-lbs				Moment, ft-lbs			
	M_x	M_y	M_z	SRSS[1]	M_x	M_y	M_z	SRSS[1]
10	7466	-3125	4903	9463	11032	-8211	7167	15508
15	5457	-2169	3947	7075	8427	-6821	5875	12331
20a	5457	-2169	3947	7075	8427	-6821	5875	12331
20b	5188	-1989	3512	6573	8030	-6561	5308	11649
25	5188	-1989	3512	6573	8030	-6561	5308	11649
30a	5188	-1989	3512	6573	8030	-6561	5308	11649
30b	3852	-1623	3821	5663	6372	-5829	5273	10119
35	3852	-1623	3821	5663	6372	-5829	5273	10119
40	-3055	-296	7572	8170	-4687	-3204	8370	10114
45	-11098	1031	11938	16332	-12778	2781	12484	18079
50a	-11098	1031	11938	16332	-12778	2781	12484	18079
50b	-13157	1397	12640	18298	-14739	2951	13196	20002
55	-13157	1397	12640	18298	-14739	2951	13196	20002
955	-10606	1397	8313	13548	-11194	2951	9633	15060
960	-8054	1397	3985	9094	-8964	2951	4863	10617
1960	-7184	1397	2509	7737	-8166	2951	4417	9742
75	-6825	1397	1901	7221	-7891	2951	4305	9461
60	-6792	1397	1843	7175	-7866	2951	4295	9436
875a	-6792	1397	1843	7175	-7866	2951	4295	9436
875b	-5327	1031	631	5462	-6577	2241	3661	7854
80	-5327	1031	631	5462	-6577	2241	3661	7854
85	-4014	605	-130	4061	-5328	1505	-3216	6403
90	-2461	178	-924	2635	-4347	1316	-5090	6822
95	1072	-248	-2842	3048	3016	-2464	-7016	8024

(1) $SRSS = \sqrt{M_x^2 + M_y^2 + M_z^2}$

Table 4-5

Moment for the 8-inch Residual Heat Removal Piping Attached to Hot Leg
(Continued)

Nodes	DW + TE				DW + TE + SSE			
	Moment, ft-lbs				Moment, ft-lbs			
	M_x	M_y	M_z	SRSS[(1)]	M_x	M_y	M_z	SRSS[(1)]
330	-2334	-378	-2254	3267	-5058	-954	-3778	6385
335	-5335	-1149	-983	5545	-7057	-1501	-1995	7486
8340a	-5335	-1149	-983	5545	-7057	-1501	-1995	7486
8340b	-7810	-1809	1112	8094	-9086	-2039	1926	9509
345	-7810	-1809	1112	8094	-9086	-2039	1926	9509
340	-7830	-1809	1311	8142	-9054	-2039	2117	9519
348	-8129	-1809	4293	9369	-9155	-2039	5467	10856
351	-8529	-1809	8268	12016	-9961	-2039	9870	14170
355	-9091	-1809	13868	16681	-10241	-2039	15196	18438
360	-9202	-1809	14961	17657	-10400	-2039	16371	19502
365	-9203	-1809	14978	17672	-10403	-2039	16390	19520
8365a	-9203	-1809	14978	17672	-10403	-2039	16390	19520
8365b	-7047	-1330	13334	15140	-7935	-1530	14326	16448
370	-7047	-1330	13334	15140	-7935	-1530	14326	16448
375	-1806	-147	7624	7836	-2852	-731	8276	8784
380	3019	1036	2355	3967	5231	2292	4353	7181
385a	3019	1036	2355	3967	5231	2292	4353	7181
385b	4772	1516	1151	5138	7580	3050	3717	8976
390	4772	1516	1151	5138	7580	3050	3717	8976
395a	4772	1516	1151	5138	7580	3050	3717	8976
395b	5470	1749	1717	5994	8574	3355	4287	10156
400	5470	1749	1717	5994	8574	3355	4287	10156
405	9433	3096	3064	10390	14039	5122	5698	15994

(1) $SRSS = \sqrt{M_x^2 + M_y^2 + M_z^2}$

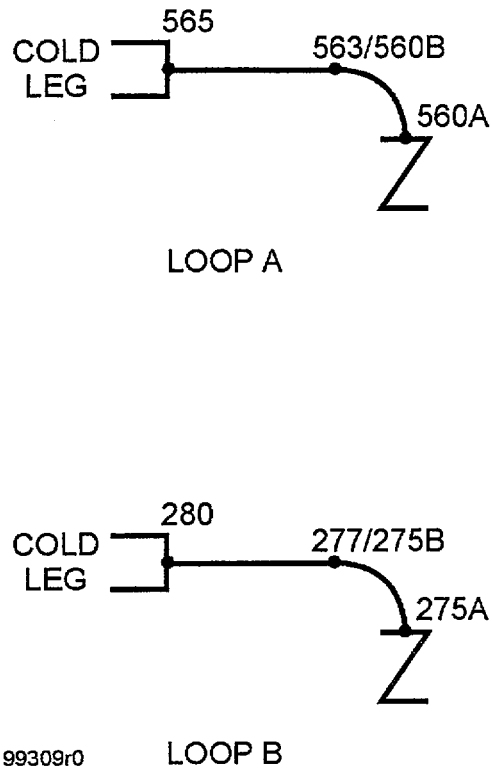

Figure 4-1. Schematic of Piping Model and Selected Node Points for the 6-inch Safety Injection Piping Attached to the Cold Leg (Loops A and B)

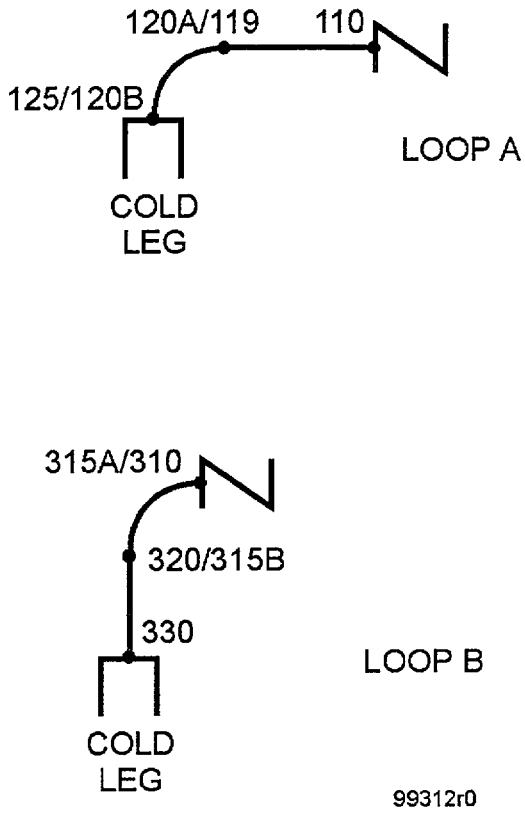

Figure 4-2. Schematic of Piping Model and Selected Node Points for the 12-inch Safety Injection Piping Attached to the Cold Leg (Loops A and B)

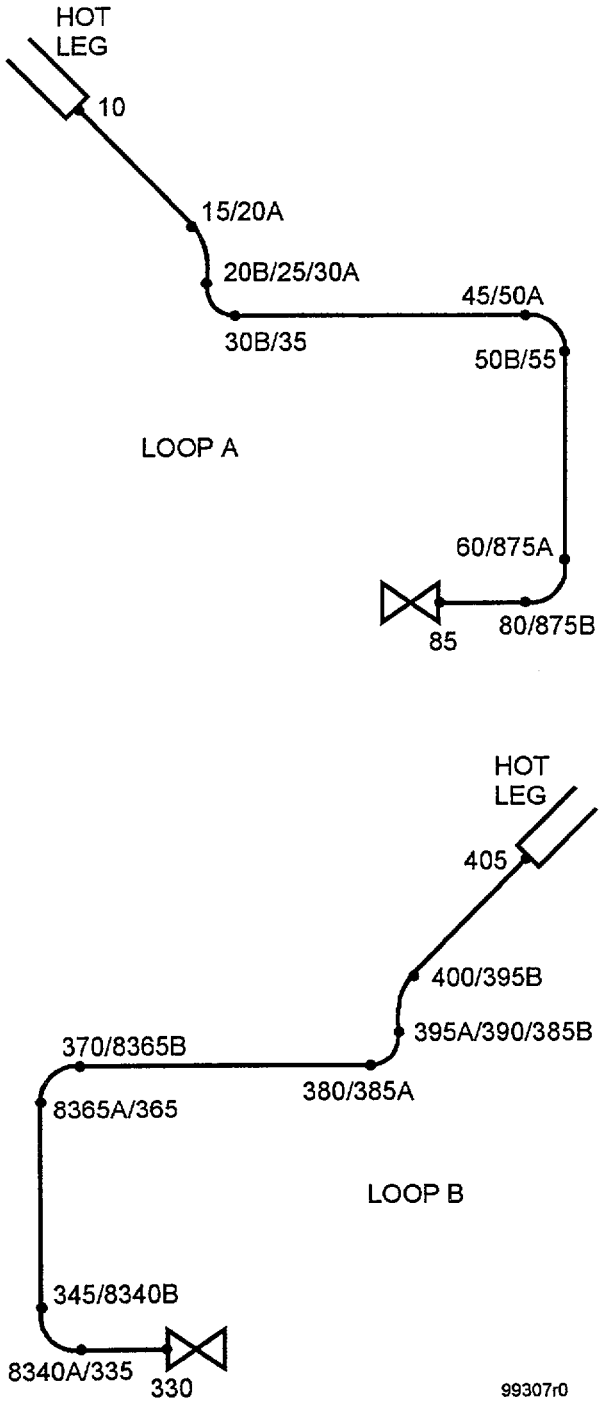

Figure 4-3. Schematic of Piping Model and Selected Node Points for the 8-inch Residual Heat Removal Piping Attached to Hot Leg (Loops A and B)

5.0 LEAK-BEFORE-BREAK EVALUATION

The LBB approach involves the determination of critical flaw sizes and leakage through flaws. The critical flaw length for a through-wall flaw is that length for which, under a given set of applied stresses, the flaw would become marginally unstable. Similarly, the critical stress is that stress at which a given flaw size becomes marginally unstable. NUREG-1061, Vol. 3 [3] defines required margins of safety on both flaw length and applied stress. Both of these criteria have been examined in this evaluation. Circumferential flaws are more restrictive than postulated axial flaws because the critical flaw sizes for axial flaw are very long since they are affected by only pressure stress and result in large crack opening areas due to out of plane displacements. For this reason, the evaluation presented herein will be based on assumed circumferential flaws.

5.1 Evaluation of Critical Flaw Sizes

Critical flaw sizes may be determined using either limit load/net section collapse criterion (NSCC) approach or J-Integral/Tearing Modulus (J/T) methodology. In this evaluation, both methods were used to determine the critical flaw sizes and the most conservative result of the two methods was chosen for a given location.

5.1.1 Critical Flaw Sizes Determined By J-Integral/Tearing Modulus Analysis

A fracture mechanics analysis for determining the stability of through-wall circumferential flaws in cylindrical geometries such as pipes using the J/T approach is presented in References 15 and 16. This procedure was used for the determination of critical stresses and flaw sizes in the safety injection and RHR lines at Kewaunee, using computer program, **pc-CRACK**™ [17] which has been verified under SI's Quality Assurance program.

The expression for the J-integral for a through-wall circumferential crack under tension loading [15] which is applied in this analysis is:

$$J = f_1\left(a_e, \frac{R}{t}\right)\frac{P^2}{E} + \alpha\sigma_o\varepsilon_o c\left(\frac{a}{b}\right)h_1\left(\frac{a}{b}, n, \frac{R}{t}\right)\left[\frac{P}{P_o}\right]^{n+1} \quad (5\text{-}1)$$

where

$$f_1\left(a_e, \frac{R}{t}\right) = \frac{a_e F^2\left(\frac{a}{b}, \frac{R}{t}\right)}{4\pi R^2 t^2} \quad (5\text{-}2)$$

a_e	=	effective crack length including small scale yielding correction
R	=	nominal pipe radius
t	=	pipe wall thickness
F	=	elasticity factor [15, 16]
P	=	applied load = σ_∞ ($2\pi Rt$); where σ_∞ is the remote tension stress in the uncracked section
α	=	Ramberg-Osgood material coefficient
E	=	elastic modulus
σ_o	=	yield stress
ε_o	=	yield strain
2a	=	total crack length
2b	=	$2\pi R$
c	=	b-a
h_1	=	plasticity factor [15, 16]
P_o	=	limit load corresponding to a perfectly plastic material
n	=	Ramberg-Osgood strain hardening exponent.

Similarly, the expression for the J-integral for a through-wall crack under bending loading [16] is given by :

$$J = f_1\left(a_e, \frac{R}{t}\right)\frac{M^2}{E} + \alpha\sigma_o\varepsilon_o c\left(\frac{a}{b}\right)h_1\left(\frac{a}{b}, n, \frac{R}{t}\right)\left[\frac{M}{M_o}\right]^{n+1} \qquad (5\text{-}3)$$

The parameters in the above equations are the same as the tension loading case except

M = applied moment = $\sigma_\infty (\pi R^2 t)$

σ_∞ = remote bending stress in the uncracked section

I = moment of inertia of the uncracked cylinder about the neutral axis

M_o = limit moment for a cracked pipe under pure bending corresponding to $n = \infty$ (elastic-perfectly plastic case)

$$= M_o'\left[\mathrm{Cos}\left(\frac{\gamma}{2}\right) - \frac{1}{2}\mathrm{Sin}(\gamma)\right] \qquad (5\text{-}4)$$

M_o' = limit moment of the uncracked cylinder = $4\sigma_o R^2 t$

The Tearing Modulus (T) is defined by the expression:

$$T = \frac{dJ}{da}\frac{E}{{\sigma_f}^2} \qquad (5\text{-}5)$$

Hence, in calculating T, J from the above expressions is determined as a function of crack size (a) and the slope of the J versus crack size (a) curve is calculated in order to determine T. (The flow stress, σ_f, is taken as the mean of the yield and ultimate tensile strengths.) The material resistance J-R curve can also be transformed into J-T space in the same manner. The intersection of the applied and the material J-T curves is the point at which instability occurs and the crack size associated with this instability point is the critical crack size.

The piping stresses consist of both tension and bending stresses. The tension stress is due to internal pressure while the bending stress is caused by deadweight, thermal and seismic loads. Because a fracture mechanics model for combined tension and bending loads is not readily available, an alternate analysis is performed to determine the critical flaw length under such loading condition

using the tension and bending models separately. For the first case, the stress combination is assumed to be entirely due to tension and the critical flaw length is determined using the tension model. For the second case, the stress combination is assumed to be entirely due to bending and the critical flaw length is determined as such. The half critical flaw sizes (lengths) obtained with the tension model (a_t) and the bending model (a_b) are combined to determine the actual half critical flaw size (a_c) due to a combined tension and bending stress using linear interpolation, as described by the following equation:

$$a_c = a_t \frac{\sigma_t}{\sigma_b + \sigma_t} + a_b \frac{\sigma_b}{\sigma_b + \sigma_t} \tag{5-6}$$

Where σ_t and σ_b are the piping tensile and bending stresses respectively.

The critical flaw sizes are determined as a function of applied moment for constant pressure stress and are presented in Tables 5-1 through 5-4. This was done so that the relationship between stress and critical flaw size can be used on a generic basis for both Kewaunee and Prairie Island. In these tables, the critical flaw length is the minimum value determined by two approaches as required by NUREG-1061, Vol. 3. In the first approach, the half critical flaw length is determined with a factor of unity on the normal + SSE stress combination. The leakage flaw total length in this case (ℓ_1) is equal to the half critical flaw length (a_c). In the second approach, critical flaw length is determined with a factor of $\sqrt{2}$ on the normal + SSE stresses. The leakage flaw length in this case (ℓ_2) is the total flaw length ($2a_c$). The final leakage flaw length is the minimum of ℓ_1 and ℓ_2. It was determined that the leakage flaw size based on a factor of unity on the stresses was controlling for all cases and as such are the values shown in Tables 5-1 through 5-4.

The fracture mechanics models used in the determination of the critical flaw sizes (lengths) are limited to flaw sizes of half the circumference of the pipe. For cases where the piping moments/stresses are relatively low, the critical flaw sizes are much greater than half the circumference of the pipe. As can be seen in Tables 5-1 through 5-4 and also Figures 5-2 through 5-5, an extrapolation scheme was used to determine the critical flaw sizes. In order to check the

validity of the extrapolation, the critical flaw sizes were also determined by limit load analysis (to be discussed in the next section) and compared to the J/T analysis results. As shown in Figures 5-2 through 5-5, the trending of the extrapolated J/T analysis results and the limit load results is very similar, demonstrating that the extrapolation method used for the J/T analysis is reasonable. Nevertheless, both the J/T analysis and limit load analysis results are presented in this evaluation.

5.1.2 Critical Flaw Sizes Determined by Limit Load Analysis

The methodology provided in NUREG-0800 [4] for calculation of critical flaw sizes by net section collapse (NSC-limit load) analysis was used to determine the critical flaw sizes. This methodology involves constructing a master curve where a stress index, SI, given by

$$SI = S + M P_m \tag{5-7}$$

is plotted as a function of postulated total circumferential through-wall flaw length, L, defined by

$$L = 2 \theta R \tag{5-8}$$

where

$$S = \frac{2 \sigma_f}{\pi} [2 \sin\beta - \sin \theta] \tag{5-9}$$

$$\beta = 0.5 [(\pi - \theta) - \pi (P_m / \sigma_f)], \tag{5-10}$$

θ = half angle in radians of the postulated throughwall circumferential flaw,

R = pipe mean radius, that is, the average between the inner and outer radius,

P_m = the combined membrane stress, including pressure, deadweight, and seismic components,

M = the margin associated with the load combination method (that is, absolute or algebraic sum) selected for the analysis. Since the moments were added algebraically, a value of 1.4 recommended in Reference 4 was used.

σ_f = flow stress for austenitic steel pipe material categories. The value of 51 ksi recommended in Reference 4 was used in this case.

If $\theta + \beta$ from Eqs. (5-9) and (5-10) is greater than π, then

$$S = \frac{2\sigma_f}{\pi}[\sin\beta], \tag{5-11}$$

where

$$\beta = -\pi\,(P_m/\sigma_f) \tag{5-12}$$

The critical flaw sizes correspond to the value of θ that result is S being greater than zero from Eqs. 5-9 and 5-11.

The value of SI used to enter the master curve for base metal and TIG welds is

$$SI = M\,(P_m + P_b) \tag{5-13}$$

where

P_b = the combined primary bending stress, including deadweight and seismic components

The value of SI used to enter the master curve for SMAW and SAW is

$$SI = M\,(P_m + P_b + P_e)\,Z \tag{5-14}$$

where

P_e = combined thermal expansion stress at normal operation,

Z = 1.15 [1.0 + 0.013 (OD-4)] for SMAW, (5-15)

Z = 1.30 [1.0 + 0.010 (OD-4)] for SAW, (5-16)

OD = pipe outer diameter in inches.

Since the loads were combined algebraically, a second evaluation was conducted with M = 1. For this case, the leakage size was determined as one half the flaw size based on the master curve. The smaller of the leakage size flaws determined from the M = 1 and M = 1.4 evaluations is the required leakage size flaw based on the limit load analysis.

In this evaluation, the SMAW parameters are used since the piping was welded using this method. The critical flaw sizes were calculated as a function of moments and presented for the various piping lines in Tables 5-5 through 5-8. These results are applicable to both Kewaunee and Prairie Island.

5.2 Leak Rate Determination

The determination of leak rate is performed using the EPRI program, PICEP [18]. The flow rate equations in PICEP are based on Henry's homogeneous nonequlibrium critical flow model [19]. The program accounts for nonequlibrium "flashing" mass transfer between liquid and vapor phases, fluid friction due to surface roughness and convergent flow paths.

In the determination of leak rates using PICEP, the following assumptions are made:

- A plastic zone correction is included. This is consistent with fracture mechanics principles for ductile materials.
- The crack is assumed to be elliptical in shape. This is the most common approach that is available in PICEP for calculations of leakage.
- Crack roughness is taken as 0.000197 inches [20].
- There are no turning losses assumed since the crack is assumed to be initiated by some mechanism other than IGSCC.

- A sharp-edged entrance loss factor of 0.61 is used (PICEP default).
- The default friction factors of PICEP are utilized.
- The stress combination used includes pressure, dead weight and thermal expansion stresses.

The leakage was calculated for an operating pressure of 2235 psig and a temperature of 550°F or 607.4°F as appropriate using location-unique moments and material properties. For each location, the leakage flaw size was determined based on the information provided in Tables 5-1 through 5-4 for EPFM analysis and also Table 5-5 through 5-8 for net section collapse analysis using the actual moments at each location. The leakage was then determined using the normal operating moment at each location. Tables 5-9 through 5-12 show the predicted leakage for the leakage flaw length for each location. In all cases, the leakage for cracks determined with net section collapse analyses was less than the leakage for cracks determined using J/T analysis. The leakage associated with net section collapse analyses is therefore conservatively used in the LBB evaluation.

5.3 Effect of Piping Restraint on LBB Evaluation

In NUREG/CR-6443 [21], a study was performed which showed that restraint of pressure induced bending in a piping system has an effect on LBB analysis results. This was shown to be especially important for small diameter piping such as those being considered for Kewaunee and Prairie Island. In this section, an evaluation is performed to assess the impact of the piping restraint on the LBB evaluation.

Recall that the above determination of critical flaw sizes and leakage rates assumes that the pipe is free to displace. With a crack in an unrestraint pipe, there is localized bending of the pipe concentrated in the crack region. This results in a "kink angle" which can be described as a change in direction of the straight pipe due to the presence of the crack. However, all the piping systems considered in this LBB evaluation are restrained to varying degrees. The opening of the crack and the resulting localized kink angle is resisted by the piping restraints, resulting in a bending moment at the crack location that is in the opposite direction of the kink angle. The presence of the restraint in a flawed piping has two effects.

1) There is a restraint of pressure induced bending for a crack in the piping system. If the pipe is free to displace, a bending moment is developed for a pipe under axial load (resulting from pressure) which is equal to the load times eccentricity (distance from center of the crack plane to the center of the pipe). In a restrained piping system, this induced bending can be restrained resulting in an increased load capacity for the flawed piping (i.e., the critical flaw size increases).

2) The restraint of the bending moment decreases the crack opening displacement and hence reduces the leakage that would have otherwise been calculated.

The effect of these two factors is what effectively introduces a bending moment in the piping system which is in opposite direction to that of the thermal restraint bending moment. This is illustrated in Figure 5-6. The uncracked pipe is shown in 5-6 (a). In 5-6 (b), the piping is shown with a crack that creates the local slope discontinuities. Here, it is assumed that there is no constraint and the piping freely displaces. In 5-6 (c), the restraint is added, causing a crack-closing moment to occur.

In LBB evaluation, the effects of restraint increasing critical flaw sizes and reducing leakage have compensating effects. However, the exact contribution of each factor cannot be easily quantified in order to determine if the results of the LBB evaluations presented above will be affected. As such, an evaluation is performed using some of the representative piping systems at Kewaunee and Prairie Island to determine the affect of restraint on the LBB evaluation results. Hence, this evaluation is applicable to both Kewaunee and Prairie Island. To select the lines to use in this analysis, a set of simple criteria was adopted.

1) Compare the similarity of the geometrical configurations of the lines

2) Use thermal anchor stresses as a measure of overall piping system restraint and select the piping lines with the highest thermal stresses at the anchor locations.

Based on the criteria above, it was concluded that all six 8-inch RHR lines are similar enough in geometry that the line with the highest thermal anchor stresses (Prairie Island Unit 1, Loop A) can be conservatively used to represent all the RHR lines. Similar conclusions were reached for the 6-inch SI lines attached to the cold leg, and hence, the Kewaunee, Loop B line was used. The 6-inch draindown line in Prairie Island Unit 2 was used for the evaluation.

The evaluation consists of first modeling the piping lines and then applying a kink angle at all weld locations from the LBB analyses. This process resulted in applied moments at each location that could be used in assessing leakage rate reduction. The three selected piping lines were modeled as PIPE16 elements using the ANSYS computer code [22]. All three models were bounded by two anchors, one of them being the connection to the RCS system. The other was placed at a significant distance away from welds of interest. The piping models used in the analysis are shown in Figures 5-7 through 5-9.

The kink angle was determined using the methodology in NUREG/CR-4572 [23], and is given by:

$$\phi = \frac{\sigma_f}{E}\left[S_b I_b(\theta_e) + S_t I_t(\theta_e)\right]\left[1 + \alpha'(S_b + S_t)^{n-1}\right] \qquad (5\text{-}17)$$

where:

σ_f = flow stress $\equiv 0.5(\sigma_u+\sigma_y)$ = Average of ultimate and yield strength of the material, ksi

E = Young's modulus in ksi,

$S_b = \sigma_b/\sigma_f$ = normalized bending stress,

$S_t = \sigma_t/\sigma_f$ = normalized tensile stress,

I_b and I_t are compliance functions given in Appendix B of Reference 23,

θ_e = effective half-crack angle corrected for plastic zone size, in radians, described below,

$\alpha' = \alpha(\sigma_f/\sigma_o)^{n-1}$

α and n are Ramberg-Osgood parameters, described below.

The plastic stress-strain behavior is represented in the Ramberg-Osgood form (Eq. 2.18 in [23]),

$$\frac{\varepsilon}{\varepsilon_o} = \frac{\sigma}{\sigma_o} + \alpha\left(\frac{\sigma}{\sigma_o}\right)^n \tag{5-18}$$

where:

σ = $\sigma_b+\sigma_t$,

σ_0 = reference stress used in determining the Ramberg-Osgood constants, usually σ_y,

ε_0 = σ_0/E,

α and n are material parameters obtained from curve-fitting to tensile test results.

The effective half-crack angle (θ_e) corrected for plastic zone size is (Eq. 2.8 in [23]):

$$\theta_e = \frac{K^2}{\pi R \sigma_f{}^2 \beta} + \theta_o \tag{5-19}$$

where:

θ_0 = a/R = original crack size,

a = circumferential crack length,

R = mean radius of the pipe,

K = stress intensity factor (Eq. 2.2 in [28]), i.e.,

$$K = \sqrt{\pi R \theta_o}\,(\sigma_t F_t(\theta_o) + \sigma_b F_b(\theta_o)) \tag{5-20}$$

F_t = geometry factor for tension (See Appendix A of Reference 23),

F_b = geometry factor for bending (See Appendix A of Reference 23),

β = 2, for plane stress condition, parameter in Irwin plastic zone correction (Eq. 2.4 in [23])

The kink angle was applied individually at all weld locations from the LBB analysis on the piping lines considered in the analysis. At each weld location, the kink angle is applied in four different directions (0°, 45°, 90°, and 135°) simulating different possible locations of a crack at that location.

The resulting moments due to the introduction of the kink angles at the various weld locations on the various lines is summarized in Tables 5-13 through 5-15. These moments act in the opposite direction to the thermal restraint moments and were therefore subtracted from the moments used in calculating the leakage rate. The resulting leakage rates for the three lines considered in this analysis are shown in Tables 5-16 through 5-18. In comparing these results to the corresponding ones without the restraint, it can be seen that the effect of the restraint did not change the leakage rate significantly for the 6-inch piping. However, the leakage for the 8-inch pipe was reduced by approximately 13%. This is a conservative estimate of leakage reduction since no credit was taken for the effects of restraint on increasing the critical flaw sizes. These results are consistent with the conclusions in a similar study in Reference 27.

5.4 LBB Evaluation Results and Discussions

It can be seen from Tables 5-9 through 5-16 that the limiting leakage is obtained from the limit load evaluation. Without the consideration of piping restraint effect, the predicted leakage range for all the lines considered in this evaluation are summarized below.

6-inch Safety Injection Lines Attached to Cold Leg	5.189 – 5.289 gpm
8-inch RHR Lines Attached to Hot Leg	7.480 – 11.276 gpm
12-inch Safety Injection Lines Attached to Cold Leg	30.128 – 31.126 gpm
6-inch Hot Leg Capped Nozzles	3.740 gpm

The piping restraint has no significant impact on the predicted leakages for the 6-inch safety injection and draindown lines. At the worst location, piping restraint produced about 13% reduction of the leak rate on the 8-inch RHR line. The minimum leakage is 7.480 gpm

associated with the 8-inch RHR piping without the consideration of the piping restraint effect. If this effect is taken into account, it is expected that the leakage would reduce to 6.51 gpm. The minimum leakage for all the systems considered in the evaluation is 3.74 gpm associated with the 6-inch hot leg nozzles. This is well above the required leak detection of 2.5 gpm for Kewaunee as discussed in Section 1.3 of this report thereby justifying LBB for all the piping considered in this evaluation.

Table 5-1

Leakage Flaw Size Versus Stress Determined by J/T Analysis for 6-inch Safety Injection Lines Attached to RCS Cold Leg (Temperature = 550°F)

Total Stress, σ_T, ksi	Bending Stress, σ_b, ksi	Tension Stress, σ_t, ksi	Bending Moment, in-kips	Leakage Flaw Size (2a), inches
3.55	0.00	3.55	0.0	2.81*
3.83	0.28	3.55	5.0	2.79*
4.11	0.56	3.55	10.0	2.77*
5.24	1.69	3.55	30.0	2.69*
6.36	2.81	3.55	50.0	2.60*
7.48	3.93	3.55	70.0	2.52*
8.60	5.05	3.55	90.0	2.44*
9.17	5.62	3.55	100.0	2.40*
9.73	6.18	3.55	110.0	2.36*
10.29	6.74	3.55	120.0	2.32*
10.85	7.30	3.55	130.0	2.27*
11.0	7.45	3.55	132.7	2.26*
12.0	8.45	3.55	150.5	2.19
13.0	9.45	3.55	168.3	2.12
14.0	10.45	3.55	186.1	2.04

*-Linearly extrapolated values

Table 5-2

Leakage Flaw Size Versus Stress Determined by J/T Analysis for 12-inch Safety Injection Lines Attached to RCS Cold Leg (Temperature = 550°F)

Total Stress, σ_T, ksi	Bending Stress, σ_b, ksi	Tension Stress, σ_t, ksi	Bending Moment, in-kips	Leakage Flaw Size (2a), inches
3.82	0.00	3.82	0.00	5.39*
4.23	0.41	3.82	50.00	5.32*
4.63	0.82	3.82	100.00	5.26*
5.45	1.63	3.82	200.00	5.14*
6.27	2.45	3.82	300.00	5.02*
7.08	3.26	3.82	400.00	4.90*
7.90	4.08	3.82	500.00	4.78*
8.71	4.90	3.82	600.00	4.66*
9.53	5.71	3.82	700.00	4.54*
10.35	6.53	3.82	800.00	4.42*
11.00	7.18	3.82	880.00	4.32*
12.00	8.18	3.82	1002.54	4.18
13.00	9.18	3.82	1125.07	4.03
14.00	10.18	3.82	1247.60	3.89
14.50	10.68	3.82	1308.86	3.82

*-Linearly extrapolated values

Table 5-3

Leakage Flaw Size Versus Stress Determined by J/T Analysis for 8-inch RHR Lines Attached to RCS Hot Leg (Temperature = 607.4°F)

Total Stress, σ_T, ksi	Bending Stress, σ_b, ksi	Tension Stress, σ_t, ksi	Bending Moment, in-kips	Leakage Flaw Size (2a), inches
4.32	0.00	4.32	0.00	3.63*
5.02	0.70	4.32	25.00	3.56*
5.72	1.40	4.32	50.00	3.49*
6.14	1.82	4.32	65.00	3.44*
6.50	2.18	4.32	77.81	3.40*
8.00	3.68	4.32	131.28	3.25*
9.00	4.68	4.32	166.93	3.14*
10.00	5.68	4.32	202.57	3.04*
11.00	6.68	4.32	238.22	2.93
11.50	7.18	4.32	256.04	2.88
12.00	7.68	4.32	273.87	2.83
12.50	8.18	4.32	291.69	2.78
14.00	9.68	4.32	345.16	2.63
15.00	10.68	4.32	380.80	2.54
16.50	12.18	4.32	434.27	2.41
17.50	13.18	4.32	469.92	2.32
18.00	13.68	4.32	487.74	2.28

*-Linearly extrapolated values

Table 5-4

Leakage Flaw Size Versus Stress Determined by J/T Analysis for 6-inch Draindown Lines and Nozzles Attached to RCS Hot Leg (Temperature = 607.4°F) (Applicable Only to Prairie Island Units 1 and 2)

Total Stress, σ_T, ksi	**Bending Stress, σ_b, ksi**	**Tension Stress, σ_t, ksi**	**Bending Moment, in-kips**	**Leakage Flaw Size (2a), inches**
3.55	0.00	3.55	0.0	2.89*
3.83	0.28	3.55	5.0	2.87*
4.11	0.56	3.55	10.0	2.85*
5.24	1.69	3.55	30.0	2.75*
6.36	2.81	3.55	50.0	2.65*
7.48	3.93	3.55	70.0	2.56*
8.60	5.05	3.55	90.0	2.46*
9.17	5.62	3.55	100.0	2.41*
9.73	6.18	3.55	110.0	2.36*
10.29	6.74	3.55	120.0	2.31*
10.85	7.30	3.55	130.0	2.27*
11.00	7.45	3.55	132.7	2.25
12.00	8.45	3.55	150.5	2.17
13.00	9.45	3.55	168.3	2.09

*-Linearly extrapolated values.

Table 5-5

Leakage Flaw Size Versus Stress Determined by Limit Load
for 6-inch Safety Injection Lines Attached to RCS Cold Leg (Temperature = 550°F)

Moment, in-kips	Leakage Flaw Size (2a), inches
0	2.710
18.6	2.619
37.2	2.534
55.8	2.452
74.5	2.377
93.1	2.304
111.7	2.236
130.3	2.170
148.9	2.106
167.5	2.044
186.1	1.986

Table 5-6

Leakage Flaw Size Versus Stress Determined by Limit Load
for 12-inch Safety Injection Lines Attached to RCS Cold Leg (Temperature = 550°F)

Moment, in-kips	Leakage Flaw Size (2a), inches
0.0	5.111
130.9	4.926
261.8	4.753
392.7	4.594
523.5	4.440
654.4	4.295
785.3	4.157
916.2	4.023
1047.1	3.895
1178.0	3.770
1308.9	3.650

Table 5-7

Leakage Flaw Size Versus Stress Determined by Limit Load
for 8-inch RHR Lines Attached to RCS Hot Leg (Temperature = 607.4°F)

Moment, in-kips	Leakage Flaw Size (2a), inches
0.0	3.414
47.4	3.274
94.8	3.143
142.2	3.020
189.6	2.903
237.0	2.795
284.4	2.689
331.8	2.588
379.2	2.491
426.6	2.396
474.0	2.306

Table 5-8

Leakage Flaw Size Versus Stress Determined by Limit Load
for 6-inch Draindown Lines and Nozzles Attached to RCS Hot Leg (Temperature = 607.4°F)
(Applicable Only to Prairie Island Units 1 and 2)

Moment, in-kips	**Leakage Flaw Size (2a), inches**
0	2.710
16.8	2.628
33.7	2.549
50.5	2.475
67.3	2.406
84.1	2.339
100.9	2.275
117.8	2.214
134.6	2.155
151.4	2.098
168.2	2.042

Table 5-9

Predicted Leakage Rates for 6-inch Safety Injection lines Attached to RCS Cold Leg

Node	Moments		EPFM Results		Net Section Collapse Results	
	NOP in-kips	NOP+SSE in-kips	Leakage Flaw Size (2a), inches	Leakage Rate, gpm	Leakage Flaw Size (2a), inches	Leakage Rate, gpm
275a	13.97	18.59	2.735	6.293	2.619	5.189
275b	16.15	21.84	2.722	6.374	2.604	5.251
277	16.15	21.84	2.722	6.374	2.604	5.251
280	16.55	22.21	2.720	6.397	2.603	5.270
560a	12.66	13.92	2.754	6.354	2.642	5.289
560b	12.91	14.56	2.751	6.353	2.639	5.282
563	12.91	14.56	2.751	6.353	2.639	5.282
565	12.83	14.47	2.752	6.348	2.639	5.278

Table 5-10

Predicted Leakage Rates for 12-inch Safety Injection Lines Attached to RCS Cold Leg

Node	Moments		EPFM Results		Net Section Collapse Results	
	NOP in-kips	NOP+SSE in-kips	Leakage Flaw Size (2a), inches	Leakage Rate, gpm	Leakage Flaw Size (2a), inches	Leakage Rate, gpm
110	718.74	736.69	4.496	38.116	4.208	30.128
112	799.40	816.49	4.400	38.238	4.125	30.498
115	938.95	956.54	4.231	38.173	3.984	31.062
119	962.10	979.99	4.202	38.066	3.961	31.126
120a	962.06	979.96	4.202	38.066	3.961	31.126
120b	1033.16	1055.32	4.112	37.615	3.887	31.106
125	1033.16	1055.32	4.112	37.615	3.887	31.106
310	810.00	825.49	4.389	38.314	4.116	30.599
315a	810.06	825.54	4.389	38.315	4.116	30.599
315b	896.38	913.54	4.283	38.272	4.026	30.888
320	896.38	913.54	4.283	38.272	4.026	30.888
330	869.00	889.06	4.312	38.160	4.051	30.736

Table 5-11

Predicted Leakage Rates for 8-inch RHR Lines Attached to RCS Hot Leg

Node	Moments		EPFM Results		Net Section Collapse Results	
	NOP in-kips	NOP+SSE in-kips	Leakage Flaw Size (2a), inches	Leakage Rate, gpm	Leakage Flaw Size (2a), inches	Leakage Rate, gpm
10	113.56	186.10	3.085	10.643	2.912	8.576
15	84.90	147.97	3.196	10.622	3.006	8.400
20a	84.90	147.97	3.196	10.622	3.006	8.400
20b	78.88	139.79	3.220	10.597	3.026	8.346
25	78.88	139.79	3.220	10.597	3.026	8.346
30a	78.88	139.79	3.220	10.597	3.026	8.346
30b	67.96	121.43	3.274	10.685	3.074	8.355
35	67.96	121.43	3.274	10.685	3.074	8.355
40	98.04	121.37	3.274	12.442	3.074	9.776
45	195.98	216.95	2.995	13.355	2.841	11.071
50a	195.98	216.95	2.995	13.355	2.841	11.071
50b	219.58	240.02	2.927	13.359	2.788	11.276
55	219.58	240.02	2.927	13.359	2.788	11.276
955	162.58	180.72	3.101	13.370	2.925	10.817
960	109.13	127.40	3.256	12.801	3.058	10.103
1960	92.84	116.90	3.287	12.339	3.086	9.667
75	86.65	113.53	3.297	12.119	3.094	9.471
60	86.10	113.23	3.298	12.099	3.095	9.453
875a	86.10	113.23	3.298	12.099	3.095	9.453
875b	65.54	94.25	3.354	11.622	3.145	8.973
80	65.54	94.25	3.354	11.622	3.145	8.973
85	48.73	76.84	3.405	11.195	3.193	8.649
90	31.62	81.86	3.390	9.933	3.179	7.637
95	36.58	96.29	3.348	9.747	3.139	7.480

Table 5-11

Predicted Leakage Rates for 8-inch RHR Lines Attached to RCS Hot Leg
(Continued)

Node	Moments		EPFM Results		Net Section Collapse Results	
	NOP in-kips	NOP+SSE in-kips	Leakage Flaw Size (2a), inches	Leakage Rate, gpm	Leakage Flaw Size (2a), inches	Leakage Rate, gpm
330	39.20	76.62	3.405	10.591	3.193	8.165
335	66.54	89.83	3.367	11.861	3.157	9.170
8340a	66.54	89.83	3.367	11.861	3.157	9.170
8340b	97.13	114.11	3.295	12.719	3.093	9.958
345	97.13	114.11	3.295	12.719	3.093	9.958
340	97.70	114.23	3.295	12.748	3.093	9.982
348	112.43	130.27	3.248	12.851	3.051	10.161
351	144.19	170.04	3.132	12.871	2.951	10.372
355	200.17	221.26	2.982	13.357	2.831	11.107
360	211.88	234.02	2.944	13.297	2.802	11.162
365	212.06	234.24	2.944	13.295	2.801	11.162
8365a	212.06	234.24	2.944	13.295	2.801	11.162
8365b	181.68	197.38	3.052	13.555	2.885	11.077
370	181.68	197.38	3.052	13.555	2.885	11.077
375	94.03	105.41	3.321	12.926	3.116	10.075
380	47.60	86.17	3.377	10.778	3.167	8.306
385a	47.60	86.17	3.377	10.778	3.167	8.306
385b	61.66	107.71	3.314	10.852	3.110	8.418
390	61.66	107.71	3.314	10.852	3.110	8.418
395a	61.66	107.71	3.314	10.852	3.110	8.418
395b	71.93	121.87	3.273	10.899	3.073	8.530
400	71.93	121.87	3.273	10.899	3.073	8.530
405	124.68	191.93	3.068	10.972	2.898	8.877

Table 5-12

Predicted Leakage Rates for 6-inch Nozzles
Attached to RCS Hot Legs

Node	Moments		EPFM Results		Net Section Collapse Results	
	NOP in-kips	NOP+SSE in-kips	Leakage Flaw Size (2a), inches	Leakage Rate, gpm	Leakage Flaw Size (2a), inches	Leakage Rate, gpm
N/A	0	0	2.894	5.073	2.710	3.740

Table 5-13

Moments Due to Kink Angle Restraint Effects for
6-inch Safety Injection Line Attached to RCS Cold Leg

Node	Crack Orientation (Degrees)	M_x [in-kips]	M_y [in-kips]	M_z [in-kips]	SRSS [in-kips]	Limiting Load Reduction Moment [in-kips]
280	0	-0.019	-0.565	-0.157	0.587	0.587
	45	-0.068	-0.492	0.230	0.547	
	90	-0.078	-0.105	0.157	0.204	
	135	-0.042	-0.178	-0.230	0.294	
275B	0	-0.011	-0.516	-0.141	0.535	0.535
	45	-0.048	-0.447	0.210	0.496	
	90	-0.057	-0.096	0.141	0.180	
	135	-0.033	-0.164	-0.210	0.269	
275A	0	-0.057	-0.478	0.046	0.484	0.487
	45	-0.107	-0.392	0.040	0.408	
	90	-0.094	-0.398	-0.046	0.412	
	135	-0.026	-0.484	-0.040	0.487	

Table 5-14

Moments Due to Kink Angle Restraint Effects for
6-inch Draindown Line Attached to RCS Hot Leg

Node	Crack Orientation (Degrees)	M_x [in-kips]	M_y [in-kips]	M_z [in-kips]	SRSS [in-kips]	Limiting Load Reduction Moment [in-kips]
7	0	0.46	-0.34	-0.06	0.57	0.57
	45	0.34	-0.26	0.14	0.45	
	90	0.03	-0.06	0.06	0.09	
	135	-0.31	-0.14	-0.14	0.36	
8	0	0.34	-0.26	-0.05	0.43	0.43
	45	0.26	-0.21	0.10	0.34	
	90	0.02	-0.06	0.05	0.08	
	135	-0.23	-0.11	-0.10	0.27	

Table 5-15

Moments Due to Kink Angle Restraint Effects for
8-inch RHR Lines Attached to RCS Hot Leg

Node	Crack Orientation (Degrees)	M_x [in-kips]	M_y [in-kips]	M_z [in-kips]	SRSS [in-kips]	Limiting Load Reduction Moment [in-kips]
2000	0	8.02	-34.58	4.32	35.77	35.77
	45	2.93	-20.83	9.43	23.05	
	90	-3.85	-15.72	-4.32	16.76	
	135	-8.41	-29.48	-9.43	32.08	
2010A	0	6.33	-23.46	3.84	24.59	24.59
	45	1.86	-14.34	5.28	15.38	
	90	-3.69	-12.93	-3.84	13.97	
	135	-7.08	-22.05	-5.28	23.73	
2010B	0	1.64	-21.86	7.17	23.05	24.91
	45	3.34	-10.12	4.53	11.59	
	90	3.07	-12.77	-7.17	14.96	
	135	1.03	-24.47	-4.53	24.91	
2020B	0	0.07	-19.21	0.00	19.21	19.21
	45	-1.81	-12.07	7.14	14.15	
	90	-2.66	-4.97	0.00	5.62	
	135	-1.94	-12.07	-7.14	14.16	
2040A	0	-0.15	-16.57	0.25	16.58	16.58
	45	0.10	-10.09	6.22	11.87	
	90	0.28	-4.12	-0.25	4.14	
	135	0.30	-10.59	-6.22	12.29	
2040B	0	-0.20	-20.16	-0.20	20.16	20.16
	45	-0.59	-13.97	6.39	15.37	
	90	-0.63	-7.38	0.20	7.40	
	135	-0.32	-13.57	-6.39	15.00	

Table 5-15

Moments Due to Kink Angle Restraint Effects for
8-inch RHR Lines Attached to RCS Hot Leg
(Continued)

Node	Crack Orientation (Degrees)	M_x [in-kips]	M_y [in-kips]	M_z [in-kips]	SRSS [in-kips]	Limiting Load Reduction Moment [in-kips]
2070A	0	0.50	-4.75	1.79	5.08	7.03
	45	1.18	-3.46	-0.50	3.68	
	90	1.21	-5.71	-1.79	6.10	
	135	0.50	-7.00	0.50	7.03	
2070B	0	1.61	-4.13	0.39	4.45	4.45
	45	1.89	-2.91	0.84	3.56	
	90	1.05	-2.49	-0.39	2.71	
	135	-0.42	-3.71	-0.84	3.81	

Table 5-16

Leakage Flaw Size and Leakages for 6-inch Safety Injection Line Attached to RCS Cold Leg Considering Restraint Effect

Node	Leakage Results without Restraint Effects				Leakage Results with Restraint Effects			
	EPFM		Limit Load		EPFM		Limit Load	
	Leakage Flaw Size (in)	Flow Rate (gpm)	Leakage Flaw Size (in)	Leakage Flow Rate (gpm)	Leakage Flaw Size (in)	Flow Rate (gpm)	Leakage Flaw Size (in)	Flow Rate (gpm)
280	2.720	6.397	2.603	5.270	2.720	6.340	2.603	5.221
275B	2.722	6.374	2.604	5.251	2.722	6.321	2.604	5.206
275A	2.735	6.293	2.619	5.189	2.735	6.245	2.619	5.148

Table 5-17

Leakage Flaw Size and Leak Rates for 8-inch RHR Line Attached to RCS Hot Leg Considering Restraint Effects

Node	Leakage Results without Restraint Effects				Leakage Results with Restraint Effects			
	EPFM		Limit Load		EPFM		Limit Load	
	Leakage Flaw Size	Flow Rate	Leakage Flaw Size	Leakage Flow Rate	Leakage Flaw Size	Flow Rate	Leakage Flaw Size	Flow Rate
	(in)	(gpm)	(in)	(gpm)	(in)	(gpm)	(in)	(gpm)
200	2.983	12.963	2.832	10.770	2.983	11.316	2.832	9.378
2010A	2.118	13.178	2.940	10.640	3.118	11.884	2.940	9.571
2010B	3.133	13.306	2.953	10.730	3.133	11.975	2.953	9.631
2020B	3.208	13.037	3.016	10.345	3.208	11.959	3.016	9.466
2040A	2.940	12.742	2.798	10.940	2.940	11.980	2.798	10.051
2040B	2.844	12.791	2.725	11.066	2.844	11.955	2.725	10.334
2070A	3.200	8.866	3.009	6.963	3.200	8.491	3.009	6.659
2070B	3.205	9.153	3.013	7.189	3.205	8.911	3.013	6.992

Table 5-18

Leakage Flaw Size and Leak Rates for 6-inch Draindown Line
Attached to RCS Hot Leg Considering Restraint Effects

Node	Leakage Results without Restraint Effects				Leakage Results with Restraint Effects			
	EPFM		Limit Load		EPFM		Limit Load	
	Leakage Flaw Size (in)	Flow Rate (gpm)	Leakage Flaw Size (in)	Leakage Flow Rate (gpm)	Leakage Flaw Size (in)	Flow Rate (gpm)	Leakage Flaw Size (in)	Flow Rate (gpm)
7	2.845	5.245	2.661	3.884	2.845	5.195	2.661	3.845
10	2.848	5.264	2.664	3.899	2.848	5.226	2.664	3.869

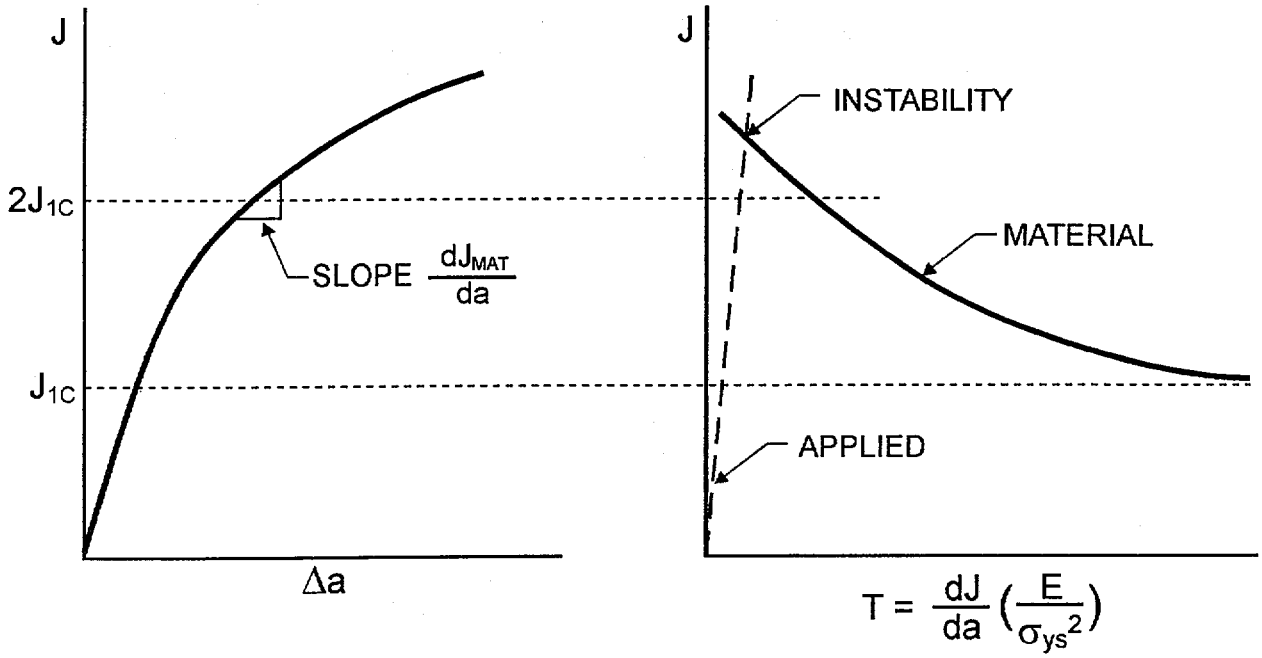

93220r0

Note: Linear extrapolation used to determine $T_{material}$ for J values greater than 2 J_{IC}

Figure 5-1. J-Integral/Tearing Modulus Concept for Determination of Instability During Ductile Tearing

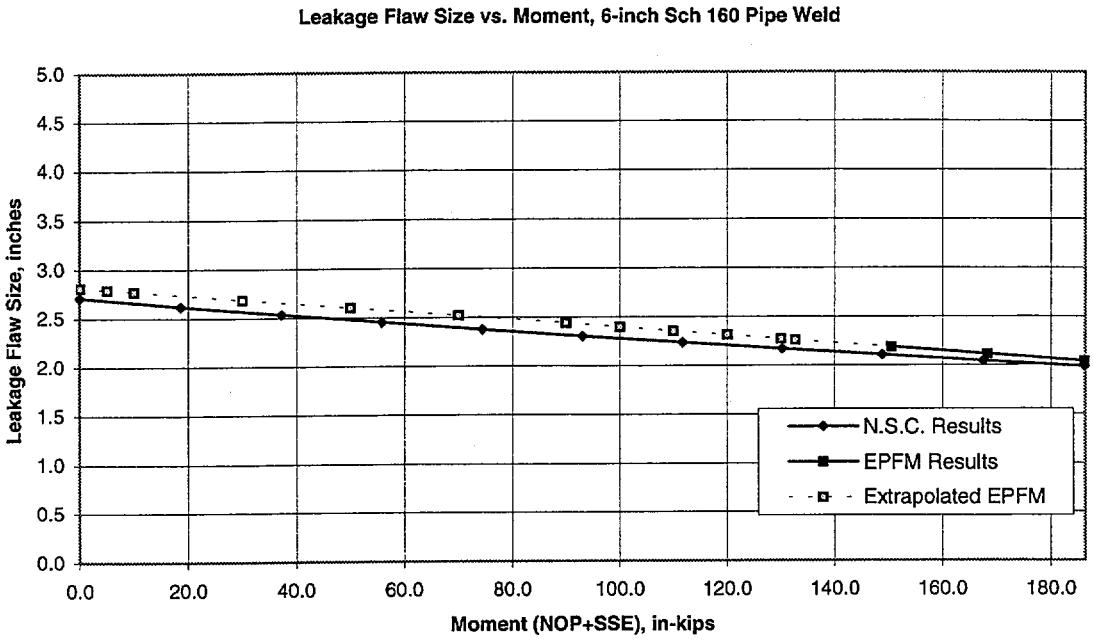

Figure 5-2. Leakage Flaw Size Versus Moment for 6-inch Schedule 160 Pipe Weld Determined by J/T and Limit Load Analyses

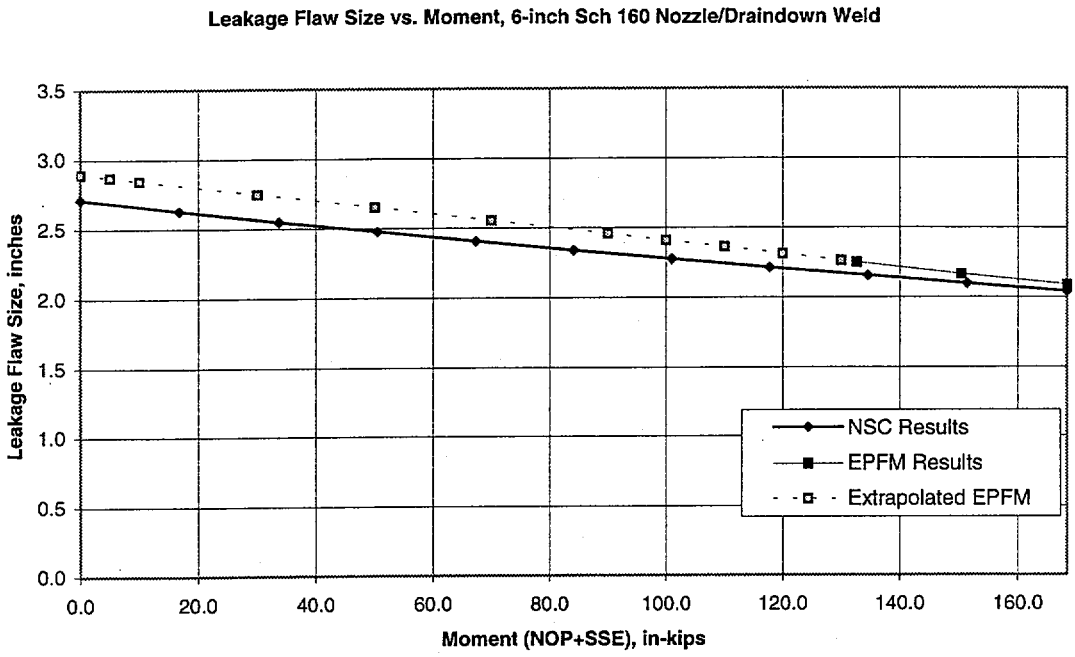

Figure 5-3. Leakage Flaw Size Versus Moment for 6-inch Schedule 160 Nozzle/ Draindown Weld Determined by J/T and Limit Load Analyses

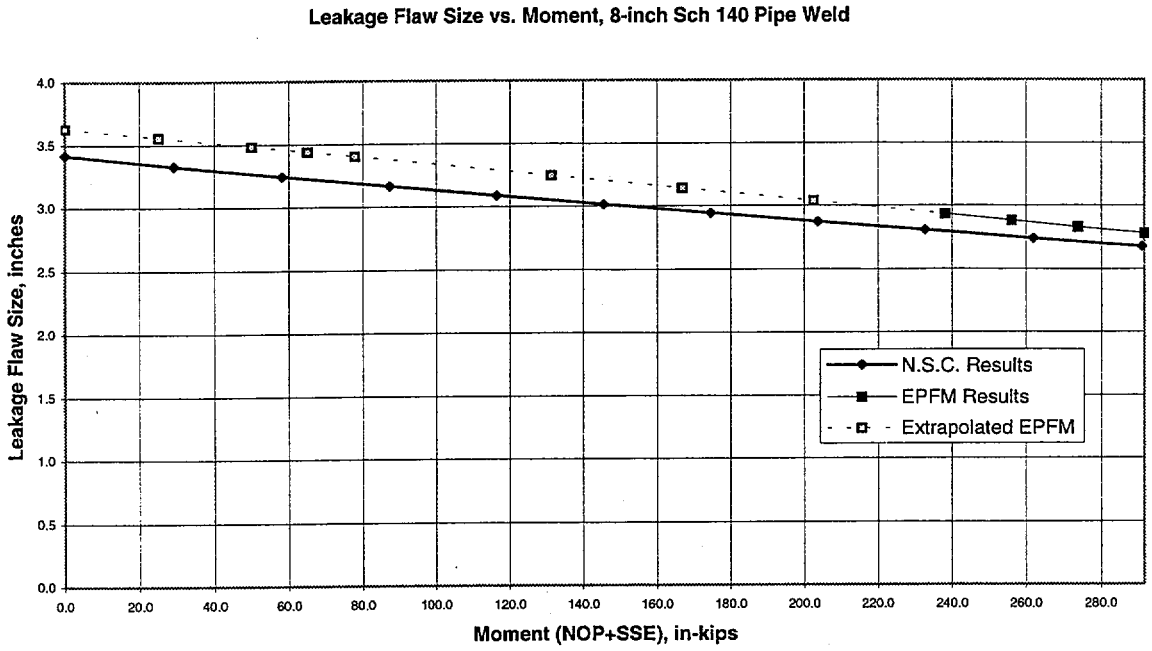

Figure 5-4. Leakage Flaw Size Versus Moment for 8-inch Schedule 140 Pipe Weld Determined by J/T and Limit Load Analyses

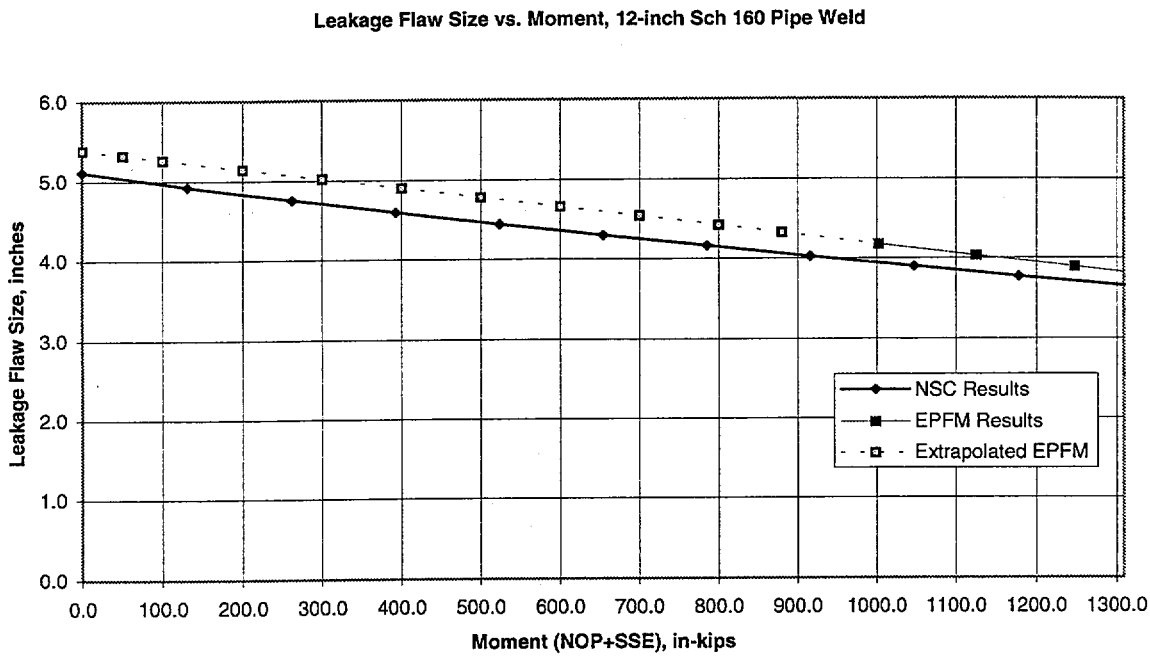

Figure 5-5. Leakage Flaw Size Versus Moment for 12-inch Schedule 160 Pipe Weld Determined by J/T and Limit Load Analyses

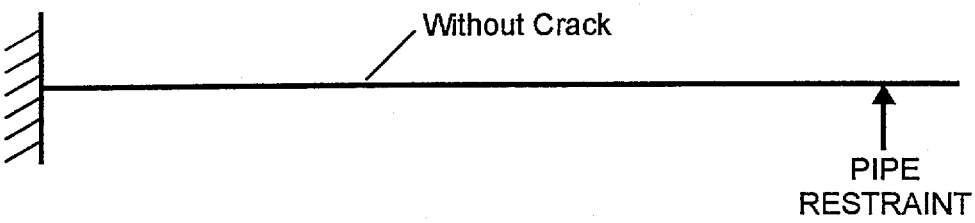

a) Uncracked piping.

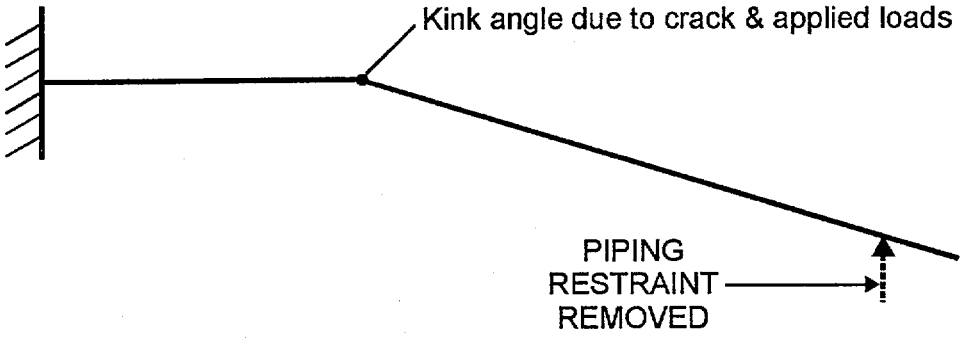

b) Cracked pipe without restraint.

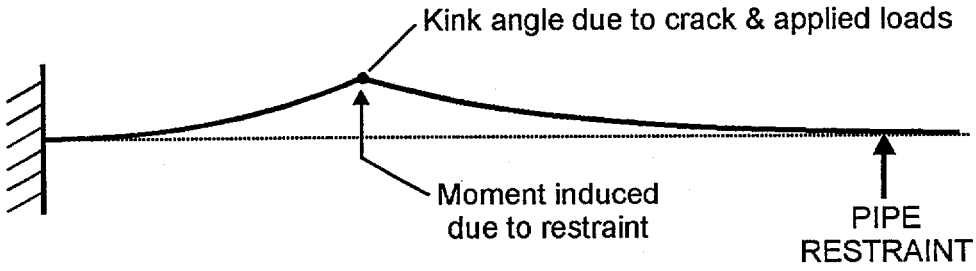

00034r0

c) Cracked pipe with restraint.

Figure 5-6. Depiction of Restraint Effect on Cracked Piping

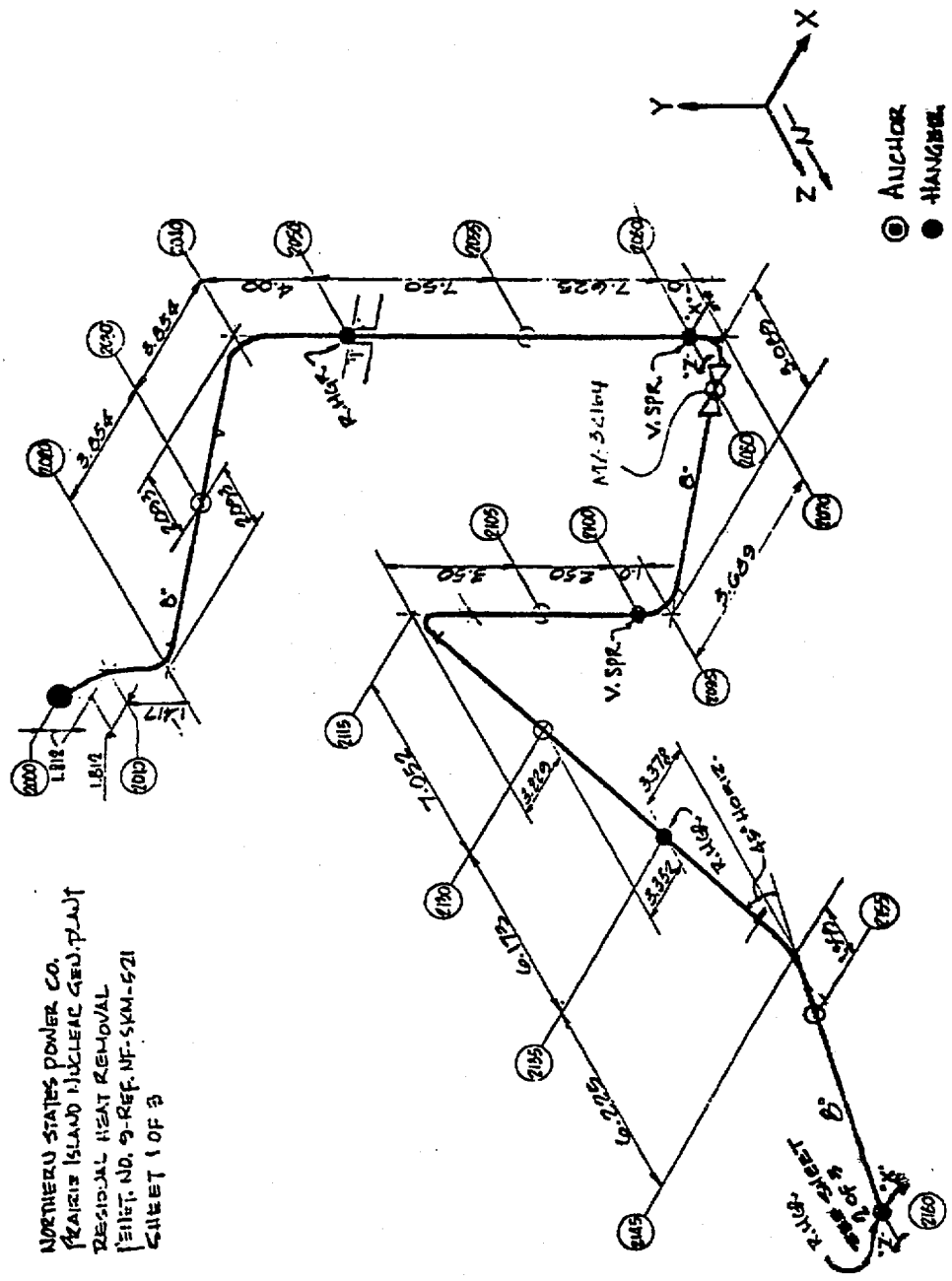

Figure 5-7. Schematic of Piping Layout Used to Determine the Effect of Restraint on LBB Evaluation (8-inch RHR Line – Prairie Island Unit 1, Loop A)

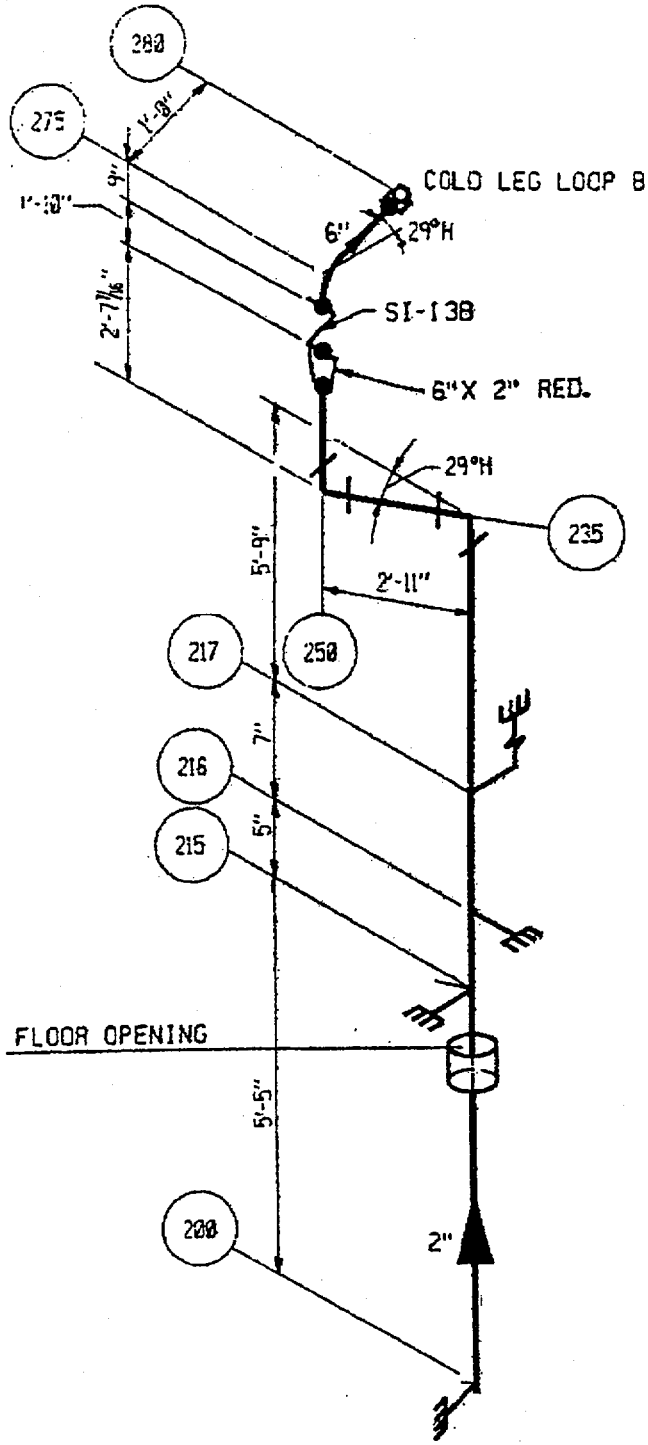

Figure 5-8. Schematic of Piping Layout Used to Determine the Effect of Restraint on LBB Evaluation (6-inch Safety Injection Line – Kewaunee, Loop B)

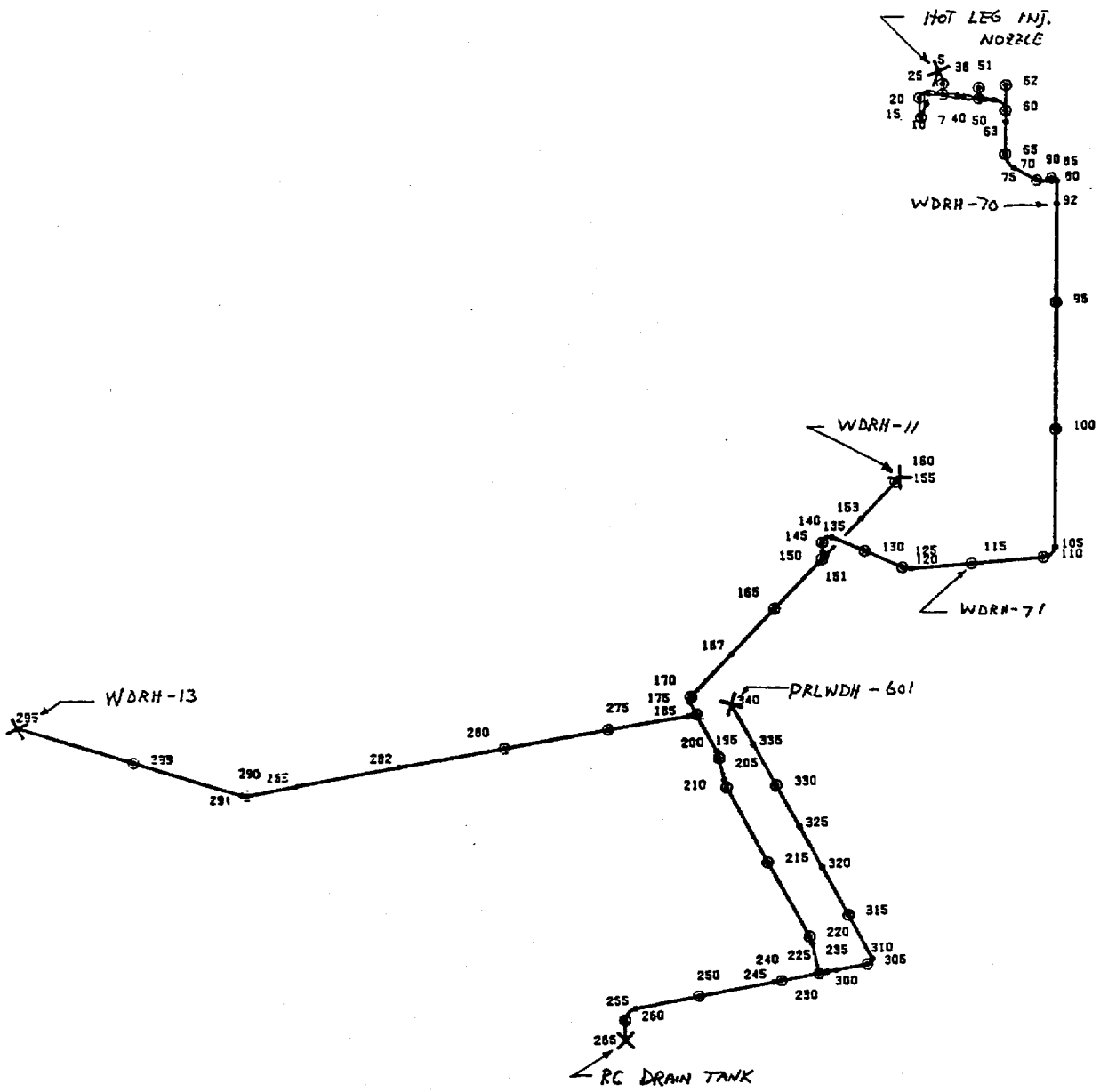

Figure 5-9. Schematic of Piping Layout Used to Determine the Effect of Restraint on LBB Evaluation (6-inch Draindown Line – Prairie Island Unit 2)

6.0 EVALUATION OF FATIGUE CRACK GROWTH OF SURFACE FLAWS

In accordance with the NRC criteria [3] set forth in Section 2 of this report, the growth of postulated surface cracks by fatigue is evaluated to demonstrate that such growth is insignificant for the plant life, when initial flaw sizes meeting ASME Code Section XI IWB-3514 acceptance standards [24] are postulated. The crack growth analysis is performed for the locations with the maximum stresses. The evaluation is performed using bounding stresses from Prairie Island Units 1 and 2 and Kewaunee such that it is applicable to all three units.

6.1 Plant Transients

Since Kewaunee RCS attached piping lines were designed to the requirements of ANSI B31.1, no specific line unique transients exist in the design basis. Hence, transient information specific only to this LBB evaluation is developed to perform the crack growth evaluation. The transients used in the evaluation consist of those specified in the Plant Technical Specification and additional transients specific to the operation of these systems. The plant transients used in this evaluation are presented in Table 6-1. These are consistent with those in the Plant Technical Specification except that the number of heatup/cooldown cycles was modified from 200 to 250 to account for future potential license renewal. The pressure change due to normal fluctuations is assumed for those events with no significant pressure change defined. Table 6-2 shows the additional thermal transients assumed for the systems. Inadvertent safety injections and accumulator blowdown transients are not evaluated, since these transients have never occurred at Kewaunee and hence are considered as very unlikely events. There are no local piping system transients for the 6-inch hot leg nozzles.

For crack growth analysis, the design basis transients are combined into load set pairs to give the largest pressure and temperature ranges. The combined transients and the associated number of cycles are shown in Table 6-3 for the hot leg and Table 6-4 for the cold leg. They are in order of decreasing ΔT except for the test events. For purposes of this analysis, the test events in Table 6-1 and the Table 6-2 transients are treated as standalone events and not combined with the normal system transients.

6.2 Stresses for Crack Growth Evaluation

The axial stresses due to pressure and thermal loads are calculated as described below. For pressure loads, P, the axial stress is calculated as:

$$\sigma_p = P\frac{D_i^{\,2}}{D_o^{\,2} - D_i^{\,2}}$$

where D_o is the outside diameter and D_i is the inside diameter of the pipe.

Bending stress is given by $\sigma_b = D_o(M)/2I$,

where

M = bending moment

I = moment of inertia

$= (\pi/64)*(D_o^{\,4}-D_i^{\,4})$

For thermal expansion moments, the maximum operating thermal moments ($M_{max\ oper}$), from Section 4, are scaled by the ratio of the transient temperature range (ΔT) to the operating temperature range (ΔT_{oper}):

$$M_t = M_{max\ oper}\ (\Delta T/\Delta T_{oper}),$$

where ΔT_{oper} is based on the temperatures at which the thermal expansion moments were calculated. $\Delta T_{oper} = 607.4 - 70 = 537.4°F$ for the hot leg and $552 - 70 = 482°F$ for the cold leg. Table 6-5 gives the bounding non-scaled moments, based on the Section 4 tables. The operating conditions used for this evaluation have been presented in Section 4.1.

Non-cyclic stresses were also considered as they affect crack growth rate. The dead weight stresses are computed from the dead weight moments presented in Table 6-5. In addition, weld

residual stresses are considered in the evaluation. The weld residual stress is conservatively represented by a pure through-wall bending stress approximately equal to the base metal material yield stress (S_y) at the operating temperature. Thus, for the cold leg, S_y = 19.3 ksi at 550°F was used while for the hot leg, S_y = 18.8 ksi at 607.4°F was used.

Thermal transient stresses (σ_{TT}) and thermal stresses associated with material discontinuities (σ_{TD}) are also included in this evaluation and are presented in Tables 6-6 and 6-7. The computer program PIPETRAN [25] was used to derive the through-wall thermal transient and discontinuity stresses for the given transients. This program performs two-dimensional axisymmetric transient thermal stress analysis for cylindrical components. This program is maintained under SI's software quality assurance program.

The axial pressure, thermal, dead weight and residual stresses were combined to obtain the stress ranges corresponding to each load group. Within a load group, the maximum stresses were used. The resulting stress ranges are shown in Tables 6-8 through 6-10 where the pressure and bending moment stresses are taken as uniform tension across the pipe thickness and the other stresses are considered to have a linear through-wall distribution.

6.3 Model for Stress Intensity Factor

The stress intensity factors, K, corresponding to the point of the maximum depth of a semi-elliptical crack are calculated using fracture mechanics solutions presented in Reference 13. The stress intensity factors are determined for a conservative aspect ratio (a/ℓ) of 0.1.

The stress intensity factor for the deepest point on the semi-elliptical flaw from Reference 13 is given as:

$$K_I = (\pi t)^{0.5} \cdot \left[\sum_{i=0}^{3} \sigma_i (a/t)^i G_i \right]$$

where σ_i are the coefficients of the stress polynomial describing the axial stress (σ) variation through the cylinder wall and are defined below.

$$\sigma = \sigma_o + \sigma_1 (z/t) + \sigma_2 (z/t)^2 + \sigma_3 (z/t)^3,$$

z is the distance measured from the inner surface of the cylinder wall and t is the cylinder wall thickness. The G_i are the influence coefficients associated with the coefficients of the stress polynomial σ_i and are expressed by the following general form:

$$G_i = A_1\alpha_i + A_2\alpha_i^2 + A_3\alpha_i^3 + A_4\alpha_i^4 + A_5\alpha_i^5 + A_6\alpha_i(R/t - 5)$$

$$\alpha_i = (a/t)/(a/c)^m$$

The values of A_1 through A_6 and m are provided in Reference 13 for each G_i. The constant R is the mean radius of the cylinder. The parameters 2c and *a* are the flaw length measured at the cylinder inner surface and flaw depth at the deepest point of the flaw, respectively.

6.4 Fatigue Crack Growth Analysis and Results

Fatigue crack growth analysis requires the use of appropriate fatigue crack growth law for the stainless steel piping. Per the recommendation of ASME Code, Section XI Task Group for Piping Flaw Evaluation [26], the fatigue crack growth law for stainless steel is given as:

$$\frac{da}{dN} = CES(\Delta K_I)^n$$

where n equals 3.3, C = 2 x 10^{-19} (in/cycle) (psi/$\sqrt{in}$), and E is the environmental factor, equal to 2 for the PWR water environment. S is a scaling parameter to account for the R ratio (K_{min}/K_{max}), and is given by:

$$S = (1.0 - 0.5\,R^2)^{-4}$$

The R ratio was calculated for each K_{max} and K_{min} for each location.

The stresses are cycled between maximum and the minimum stress conditions shown in Tables 6-2 through 6-4. For each location, the actual K values for the fatigue crack growth are calculated based on the stresses.

The initial flaw size is linearly interpolated based on the allowable flaw sizes for various thicknesses from Table IWB-3514-2, Inservice Examination, surface crack, for a crack with aspect ratio a/ℓ = 0.15. However, for the crack growth analysis, an aspect ratio of 0.1 has been conservatively used. The crack depths used as input are presented in Table 6-11.

The results of the fatigue crack growth analysis are presented in Table 6-12. The results show that for the 6-inch cold leg safety injection piping, crack growth is very minimal. After 250 heatup/cooldown cycles, the crack depth is significantly below the ASME Section XI Code allowables. It should be noted that the results for the 6-inch cold leg safety injection piping can be conservatively applied to the 6-inch capped nozzle on the hot leg since only pressure stresses exist at the capped nozzle.

However, for the 12" Sch 160 SI Accumulator line, it takes 38 heatup/cooldowns at the worst location to reach the allowable flaw size. For the 8" Sch 140 RHR Suction line, it takes 123 heatup/cooldowns at the most critical location to reach the allowable flaw size. The relatively few number of cycles for the 8-inch RHR and 12" safety injection accumulator piping can be attributed to the RHR transients listed in Table 6-2. For the last ten years, Kewaunee has experienced 13 heatup/cooldown cycles which are significantly less than the minimum allowable number of 38 calculated at the most critical location. Given that the piping is inspected in accordance with ASME Section XI requirements in each 10-year interval, it is believed that the potential for crack growth can be managed by the current in-service inspection program at Kewaunee.

Table 6-1

Plant Design Transients Used for LBB Evaluations

Event	Cycles	Hot Leg			Cold Leg			P_{min}, psig	P_{max}, psig	ΔP, psi
		T_{min}, °F	T_{max}, °F	ΔT, °F	T_{min}, °F	T_{max}, °F	ΔT, °F			
Plant Heatup/Cooldown (HU/CD)	250	70	547	477	70	547	477	0	2235	2235
Plant Loading/Unloading	18,300	547	596	49	532.2	547	14.8	2135	2335	200
10% Step Load Decrease	2,000	585	601	16	531.2	547.2	16	2135	2335	200
10% Step Load Increase	2,000	591	606	15	517.2	533.2	16	2135	2335	200
Large Step Decrease	200	516	602	86	522.2	546.2	24	2135	2335	200
Loss of Load	80	536	624	88	536.2	572.2	36	2135	2335	200
Loss of Power	40	576	616	40	530.2	542.2	12	2135	2335	200
Loss of Flow	80	486	602	116	489.2	532.2	43	1855	2235	380
Reactor Trip from Full Power	400	520	596	76	522.2	535.2	13	2135	2235	2235
Turbine Roll Test	10	480	547	67	480	547	67	1935	2235	300
Primary Side Hydro Test	5	120	120	0	120	120	0	0	3105	3105
Primary Side Leak Test	50	120	547	427	120	547	427	0	2485	2485
Operating Basis Earthquake (±)	200									

Table 6-2

Additional System Transients Used Specifically for LBB Evaluations

Piping	Transient	Cycles	T_{min}, °F	T_{max}, °F	ΔT, °F
6" Cold Leg SI	High Head Safety Injection	10	32	560	528
12" SI Accumulator	RHR Operation at Cooldown	250	100	400	300
12" SI Accumulator	Refueling Floodup	120	50	150	100
8" RHR Suction	RHR Initiation (away from RC nozzle)	250	100	400	300

Table 6-3

Combined Transients for Crack Growth, Hot Leg

No.	Load Set Pair	Cycles	T_{min}, °F	T_{max}, °F	ΔT, °F	P_{min}, psig	P_{max}, psig	ΔP, psi
1	CD & HU/Loss of Load/OBE	20	70	624	554	0	2335	2335
2	CD & HU/Loss of Load	60	70	624	554	0	2335	2335
3	CD & HU/Loss of Power	40	70	616	546	0	2335	2335
4	CD & HU/10% Load Increase	130	70	606	536	0	2335	2335
5	TR Test & 10% Load Increase	10	480	606	126	1935	2335	400
6	Loss of Flow & 10% Load Increase	80	486	606	120	1855	2235	380
7	Step Decr. & 10% Load Increase	200	516	606	90	2135	2335	200
8	Rx Trip & 10% Load Increase	400	520	606	86	2135	2335	200
9	Unload & Load/10% Load Increase	1180	547	606	59	2135	2335	200
10	Unload & Load/10% Load Decrease	2000	547	601	54	2135	2335	200
11	Loading/Unloading	15120	547	596	49	2135	2335	200
12	Primary Side Hydro Test	5	120	120	0	0	3105	3105
13	Primary Side Leak Test	50	120	547	427	0	2485	2485

Table 6-4

Combined Transients for Crack Growth, Cold Leg

No.	Load Set Pair	Cycles	T_{min}, °F	T_{max}, °F	ΔT, °F	P_{min}, psig	P_{max}, psig	ΔP, psi
1	CD & HU/Loss of Load/OBE	20	70	572.2	502.2	0	2335	2335
2	CD & HU/Loss of Load	60	70	572.2	502.2	0	2335	2335
3	CD & HU	170	70	547	477	0	2235	2235
4	Turbine Roll Test Range	10	480	547	67	1935	2335	400
5	Flow Loss & 10% Load Decrease	80	489.2	547.2	58	1855	2335	480
6	10% Load Incr. & 10% Load Decr.	1920	517.2	547.2	30	2135	2335	200
7	10% Load Incr & Load/Unload	80	517.2	547	29.8	2135	2335	200
8	Reactor Trip & Load/Unload	400	522.2	547	24.8	2135	2335	200
9	Large Step Decrease & Load/Unload	200	522.2	547	24.8	2135	2335	200
10	Loading/Unloading Range	17620	532.2	547	14.8	2135	2335	200
11	Loss of Power Range	40	530.2	542.2	12	2135	2335	200
12	Primary Side Hydro Test	5	120	120	0	0	3105	3105
13	Primary Side Leak Test	50	120	547	427	0	2485	2485

Table 6-5

Bounding Moments

Line	Plant	Node	TE Moment, ft-lb			DW Moment, ft-lb			OBE Moment, ft-lb		
			M_x	M_y	M_z	M_x	M_y	M_z	M_x	M_y	M_z
6" Sch 160 Cold Leg SI	Kewaunee	280	750	254	941	-518	-2	395	102	65	211
	PI Unit 2	826	-846	49	-252	-4	-2	1	76	11	54
12" Sch 160 SI Accumulator	Kewaunee	125	-6207	37869	-76432	706	-946	-1151	708	1744	109
	Kewaunee	310	53964	-28733	32398	-1752	254	-474	331	520	356
	PI Unit 1	855	46008	-11027	-18203	2559	-476	-2946	4894	809	5269
	PI Unit 1	910	-34147	-27905	-1668	-1102	-400	-3334	3322	1620	6171
8" Sch 140 RHR Suction	PI Unit 1	2000	2967	-4507	16159	-142	-216	-1161	667	1892	396
	PI Unit 1	2324	7449	-2958	-4764	-763	278	-2078	2551	425	4261
	PI Unit 2	246	-1295	-6489	-1932	-825	10	1622	4857	1661	15274
	PI Unit 2	255A	7466	-8370	32915	51	-6	367	733	1390	1588
	PI Unit 2	270	7719	3075	5261	1775	-53	-868	445	3167	12240
6" Sch 160 Draindown	PI Unit 1	730	-355	81	184	-528	-2	410	117	276	275

Table 6-6

Maximum and Minimum Transient and Discontinuity Stress

Transition	Transient	Stress, ksi
6" SI Line to CL Nozzle	High Head Safety Injection	100.23
6" SI Line to CL Nozzle	High Head Safety Injection	-67.87
12" SI Line to CL Nozzle	RHR Operation at Cooldown	65.09
12" SI Line to CL Nozzle	RHR Operation at Cooldown	-1.96
12" SI Line to CL Nozzle	Inadvertent Accumulator Blowdown	53.45
12" SI Line to CL Nozzle	Inadvertent Accumulator Blowdown	-59.08
12" SI Line to CL Nozzle	Refueling Floodup	20.93
6" SI Line to Valve	High Head Safety Injection	124.05
6" SI Line to Valve	High Head Safety Injection	-99.03
12" SI Line to Valve	RHR Operation at Cooldown	69.56
12" SI Line to Valve	RHR Operation at Cooldown	-0.50
12" SI Line to Valve	Inadvertent Accumulator Blowdown	78.20
12" SI Line to Valve	Inadvertent Accumulator Blowdown	-82.54
12" SI Line to Valve	Refueling Floodup	24.84
8" RHR Line to Valve	RHR Initiation	-57.24

Table 6-7

Maximum and Minimum Transient Stress

Transition	Transient	Stress, ksi
6" SI Line to CL Nozzle	High Head Safety Injection	96.60
6" SI Line to CL Nozzle	High Head Safety Injection	-64.80
12" SI Line to CL Nozzle	RHR Operation at Cooldown	65.09
12" SI Line to CL Nozzle	RHR Operation at Cooldown	-2.08
12" SI Line to CL Nozzle	Inadvertent Accumulator Blowdown	52.72
12" SI Line to CL Nozzle	Inadvertent Accumulator Blowdown	-58.36
12" SI Line to CL Nozzle	Refueling Floodup	20.82
6" SI Line to Valve	High Head Safety Injection	96.28
6" SI Line to Valve	High Head Safety Injection	-64.66
12" SI Line to Valve	RHR Operation at Cooldown	64.85
12" SI Line to Valve	RHR Operation at Cooldown	-2.05
12" SI Line to Valve	Inadvertent Accumulator Blowdown	52.64
12" SI Line to Valve	Inadvertent Accumulator Blowdown	-58.28
12" SI Line to Valve	Refueling Floodup	20.84
8" RHR Line to Valve	RHR Initiation	-36.13

Table 6-8

Total Constant (σ_0) and Linear (σ_1) Through-Wall Stresses, 6" Sch 160 Cold Leg SI

Load Set Pair	Cycles	Stresses (psi)			
		Minimum		Maximum	
		σ_0	σ_1	σ_0	σ_1
CD & HU/Loss of Load/OBE	20	19395	-53760	24268	-53760
CD & HU/Loss of Load	60	19397	-53760	24109	-53760
CD & HU	170	19402	-53760	23912	-53760
Turbine Roll Test Range	10	23178	-53760	23928	-53760
Flow Loss & 10% Load Decrease	80	23067	-53760	23928	-53760
10% Load Incr. & 10% Load Decr.	1920	23559	-53760	23928	-53760
10% Load Incr & Load/Unload	80	23559	-53760	23928	-53760
Reactor Trip & Load/Unload	400	23568	-53760	23928	-53760
Large Step Decrease & Load/Unload	200	23568	-53760	23928	-53760
Loading/Unloading Range	17620	23585	-53760	23928	-53760
Loss of Power Range	40	23583	-53760	23921	-53760
Primary Side Hydro Test	5	19746	-53760	24674	-53760
Primary Side Leak Test	50	19488	-53760	24166	-53760

Table 6-9

Total Constant (σ_0) and Linear (σ_1) Through-Wall Stresses, 12" Sch 160 SI Accumulator

Load Set Pair	Cycles	Stresses (psi)			
		Minimum		Maximum	
		σ_0	σ_1	σ_0	σ_1
CD & HU/Loss of Load/OBE	20	19134	-29421	30357	-29421
CD & HU/Loss of Load	60	19134	-29421	30337	-29421
CD & HU	170	19134	-29421	29812	-29421
Turbine Roll Test Range	10	28204	-29421	29829	-29421
Flow Loss & 10% Load Decrease	80	28196	-29421	29832	-29421
10% Load Incr. & 10% Load Decr.	1920	29068	-29421	29832	-29421
10% Load Incr & Load/Unload	80	29068	-29421	29829	-29421
Reactor Trip & Load/Unload	400	29139	-29421	29829	-29421
Large Step Decrease & Load/Unload	200	29139	-29421	29829	-29421
Loading/Unloading Range	17620	29279	-29421	29829	-29421
Loss of Power Range	40	29251	-29421	29761	-29421
Primary Side Hydro Test	5	19841	-29421	25145	-29421
Primary Side Leak Test	50	19837	-29421	30085	-29421
Refueling Floodup	80	18855	-29421	49346	-79101
RHR Operation at Cooldown	250	19056	-28421	94359	-168541

Table 6-10

Total Constant (σ_0) and Linear (σ_1) Through-Wall Stresses, 8" Sch 140 RHR Suction

Load Set Pair	Cycles	Stresses (psi)			
		Minimum		Maximum	
		σ_0	σ_1	σ_0	σ_1
CD & HU/Loss of Load/OBE	20	19147	-47537	27393	-47537
CD & HU/Loss of Load	60	19504	-47537	27377	-47537
CD & HU/Loss of Power	40	19504	-47537	27184	-47537
CD & HU/10% Load Increase	130	23243	-47537	27146	-47537
TR Test & 10% Load Increase	10	25483	-47537	27146	-47537
Loss of Flow & 10% Load Increase	80	26059	-47537	27146	-47537
Step Decr. & 10% Load Increase	200	26235	-47537	27146	-47537
Rx Trip & 10% Load Increase	400	26258	-47537	27146	-47537
Unload & Load/10% Load Increase	1180	26416	-47537	27146	-47537
Unload & Load/10% Load Decrease	2000	26416	-47537	27118	-47537
Loading/Unloading	15120	26417	-47537	27090	-47537
Primary Side Hydro Test	5	20149	-47537	26146	-47537
Primary Side Leak Test	50	19807	-47537	28299	-47537
RHR Operation at Cooldown	250	-37688	66943.1	22639	-47537

Table 6-11

Initial Crack Depths for Various Locations

	t (in.)	a/t	a (in.)
6" Sch 160 Cold Leg SI	0.718	0.1163	0.0835
12" Sch 160 SI Accumulator	1.312	0.1091	0.1432
8" Sch 140 RHR Suction	0.812	0.1146	0.0930

Table 6-12

Results of Fatigue Crack Growth Analysis

	Assumed Initial Depth (in.)	Final Depth (in.)	Code Allowable Depth (in.)	Calculated Heatup/Cooldown Cycles to Reach Allowable Depth
6" Sch 160 Cold Leg SI	0.0835	0.0839	0.5385	> 250
12" Sch 160 SI Accumulator	0.1432	0.984	0.984	38
8" Sch 160 RHR Suction	0.0930	0.609	0.609	123

7.0 SUMMARY AND CONCLUSIONS

Leak-before-break (LBB) evaluations are performed for the RCS attached piping at Kewaunee Units 1 in accordance with the requirements of NUREG-1061. The evaluation included portions of the safety injection and the residual heat removal systems. The nominal pipe sizes range from 6 inches to 12 inches. The analysis has been performed using conservative generic material properties for the base metals and weldments and location specific stresses consisting of pressure deadweight, thermal and seismic loads. In the evaluations, circumferential flaws have been considered since they are more limiting than axial flaws. Critical flaw sizes and leakage flaw sizes were calculated on a location specific basis using both elastic-plastic J-Integral/Tearing modulus and limit load analyses. The most limiting critical flaw size at each location from these two analyses methods has been used in the LBB evaluation. The leakage flaw size is defined as the minimum of one half the critical flaw size with a factor of one on the stresses or the full critical flaw size with a factor of $\sqrt{2}$ on the stresses. Leakage was then calculated through the leakage flaw size. Because all the piping is of relatively small diameter, the effect of piping restraint was considered in the LBB evaluation. Fatigue crack growth analysis was also performed to determine the extent of growth of any pre-existing flaws.

Based on these evaluations, the following conclusions can be made.

- Without the consideration of piping restraint effect, the predicted leakage range for all the lines considered in this evaluation are summarized below:

6-inch Safety Injection Lines Attached to Cold Leg	5.189 – 5.289 gpm
8-inch RHR Lines Attached to Hot Leg	7.480 – 11.276 gpm
12-inch Safety Injection Lines Attached to Cold Leg	30.128 – 31.126 gpm
6-inch Hot Leg Capped Nozzles	3.740 gpm

- The piping restraint effects have no significant impact on the predicted leakages for the 6-inch safety injection and 8-inch RHR lines. At the worst location, piping restraint produces about 13% reduction of the leak rate on the 8-inch RHR line.

- The lowest predicted leakage for the safety injection and RHR lines considered in this evaluation is 3.74 gpm (the 6-inch nozzle attached to the RCS hot leg) without consideration of the piping restraint effect. When the restraint effect is considered, the minimum leakage for all the piping systems considered is still 3.74 gpm since piping restraint has no affect on the 6-inch piping.

- Based on the capability of all the available leak detection systems, Kewaunee is capable of detecting leak rates as low as 0.13 gpm. However, for this evaluation a detectable leak rate of 0.25 gpm is assumed based on previous NRC approval for a sister plant. When the NUREG-1061 margin of 10 is applied to this rate, Kewaunee leak detection capability is 2.5 gpm. The minimum predicted leakage of 3.74 gpm is greater than the leak detection at Kewaunee hence justifying leak-before-break for all the systems considered.

- Fatigue crack growth of an assumed subsurface flaw of 11% of pipe wall shows that fatigue crack growth can be managed by the current Section XI inservice inspection program at Kewaunee and therefore does not invalidate the application of leak-before-break evaluation of the safety injection and RHR lines under consideration.

- The effect of degradation mechanisms which could invalidate the LBB evaluations were considered in the evaluation. It was determined that there is no potential for water hammer, intergranular stress corrosion cracking (IGSCC) and erosion-corrosion for portions of the safety injection and RHR systems considered in the LBB evaluations.

8.0 REFERENCES

1. Structural Integrity Associates Report No. SIR-99-147, Rev. 0 "Leak-Before-Break Evaluation, 6-inch to 12-inch Safety Injection and Residual Heat Removal Piping Attached to the RCS, Prairie Island Nuclear Generating Station Units 1 and 2."

2. Stello, Jr., V., "Final Broad Scope Rule to Modify General Design Criterion 4 of Appendix A, 10 CFR Part 50," NRC SECY-87-213, Rulemaking Issue (Affirmation), August 21, 1987.

3. NUREG-1061, Volumes 1-5, "Report of the U. S. Nuclear Regulatory Commission Piping Review Committee," prepared by the Piping Review Committee, NRC, April 1985.

4. NUREG-0800, "U.S. Nuclear Regulatory Commission Standard Revision Plan, Office of Nuclear Reactor Regulation, Section 3.6.3, Leak-Before-Break Evaluation Procedure," August 1987.

5. Kewaunee Nuclear Power Plant USAR, Rev. 14, Section 6.5, "Leakage Detection and Provisions for the Primary and Auxiliary Coolant Loops."

6. Letter from G. S. Vissing (USNRC) to R. C. Mecredy (RG&E) including Safety Evaluation Report, "Staff Review of the Submittal by Rochester Gas and Electric Company to Apply Leak-Before-Break Status to Portions of the R. E. Ginna Nuclear Power Plant Residual Heat Removal System Piping (TAC No. MA039)," dated February 25, 1999, Docket No. 50-244.

7. NUREG-0927, "Evaluation of Water Hammer Occurrence in Nuclear Power Plants," Revision 1.

8. W. S. Hazelton and W. H. Koo, "Technical Report on Material Selection and Processing Guidelines for BWR Coolant Pressure Boundary Piping," NUREG-0313, Rev. 2, USNRC, January 1988.

9. U. S. Nuclear Regulatory Commission, Bulletin 88-08, "Thermal Stresses in Piping Connected to Reactor Coolant Systems," June 22, 1998 (Plus Supplements 1, 2 and 3).

10. FLUOR Engineering Inc. Calculations for Wisconsin Public Service Corporation, Kewaunee Nuclear Power Plant, Project No. 834823.

    a) Stress Report No. SI-33-007, Analytical Part No. SI-33-007, Rev. 0, "Safety Injection Piping System," December 1988.

    b) Stress Report No. SI-33-006, Analytical Part No. SI-33-006, Rev. 1, August 1989.

c) Stress Report No. SI-33-004, Analytical Part No. SI-33-004, Rev. 3, "Safety Injection System," July 1995.

d) Stress Report No. RHR-34-001, Analytical Part No. RHR-34-001, Rev. 1, "Residual Heat Removal Piping System," December 1989.

e) Stress Report No. SI-33-003, Analytical Part No. SI-33-003, Rev. 0A, May 1989.

11. Design Parameters for Replacement SG (Model 54F), Provided by Mr. C. A. Tomes (Wisconsin Public Service Corporation) to Mr. D. A. Gerber (Structural Integrity Associates) on September 15, 1999.

12. NSP Document SS-M327, Sheet 52A, "Standard Specification – Mechanical, "Piping Design Tables," Rev. 5-22-72.

13. EPRI Report No. NP-6301-D "Ductile Fracture Handbook," June 1989.

14. Chopra, O.K., "Estimation of Fracture Toughness of Cast Stainless Steels during Thermal Aging in LWR Systems," NUREG/CR-4513, ANL-93/22, Rev. 1.

15. Kumar, V., et al., "An Engineering Approach for Elastic-Plastic Fracture Analysis," EPRI NP-1931, Electric Power Research Institute, Palo Alto, CA, July 1981.

16. Kumar, V., et al., "Advances in Elastic-Plastic Fracture Analysis," EPRI NP-3607, Electric Power Research Institute, Palo Alto, CA, August 1984.

17. Structural Integrity Associates, Inc., "**pc-CRACK**™ Fracture Mechanics Software," Version 3.0 - 3/27/97.

18. EPRI Report NP-3596-SR, "PICEP: Pipe Crack Evaluation Computer Program," Rev. 1, July 1987.

19. P.E. Henry, "The two-Phase Critical Discharge of Initially Saturated or Subcooled Liquid," Nuclear Science and Engineering, Vol. 41, 1970.

20. EPRI Report NP-3395, "Calculation of Leak Rates Through Crack in Pipes and Tubes," December 1983.

21. NUREG/CR-6443, BMI-2191, "Deterministic and Probabilistic Evaluation for Uncertainty in Pipe Fracture Parameters in Leak-Before-Break and in Service Flow Evaluations," June 1996.

22. ANSYS LinearPlus/Thermal, Revision 5.5.1, ANSYS, Inc., October 1998.

23. NUREG/CR-4572, BMI-2134, "NRC Leak-Before-Break (LBB.NRC) Analysis Method for Circumferentially Through-Wall Cracked Pipes Under Axial Plus Bending Loads," May 1986.

24. ASME Boiler and Pressure Vessel Code, Section XI, 1989 Edition.

25. PIPETRAN, Version 2.0, Structural Integrity Associates, Inc., 4/8/99.

26. ASME Section XI Task Group for Piping Flaw Evaluation, "Evaluation of Flaws in Austenitic Steel Piping," Journal of Pressure Vessel Technology, Vol. 108, August 1986, pp. 352-366.

27. E. Smith, "The Effect of System Flexibility on the Formulation of a Leak Before Break Case for Cracked Piping," Proceedings, ASME Pressure Vessel and Piping Conference, PVP - Vol. 313-1, Codes and Standards, Vol. 1, 1995.

APPENDIX A

DETERMINATION OF RAMBERG-OSGOOD PARAMETERS AT 650°F

A.1 INTRODUCTION

The Ramberg-Osgood stress-strain parameters (α and n) are necessary for elastic-plastic fracture mechanics analysis. These parameters may be a function of temperature. This section provides the methodology for making adjustment for the Ramberg-Osgood stress-strain parameters at a different temperature when the parameters for another temperature are known. In this case, the Ramberg-Osgood parameters are derived for at 650°F for given values at 550°F for the Type 316 stainless steel piping SMAW welds at Prairie Island and Kewaunee.

A.2 METHODOLOGY

The Ramberg-Osgood model is in the form:

$$\frac{\varepsilon}{\varepsilon_o} = \frac{\sigma}{\sigma_o} + \alpha\left[\frac{\sigma}{\sigma_o}\right]^n \qquad (1)$$

Where σ and ε are the true stress and true strain, σ_o and ε_o are the reference stress and reference strain (in general yield stress and yield strain) and α and n are the so called Ramberg-Osgood (R-O) parameters.

When the stress-strain curve at the temperature of interest is available, the R-O parameters can be obtained by curve fitting over the strain range of interest. In the absence of the stress-strain curve of the material, a methodology for determining the R-O parameters based on ASME Code-specified mechanical properties is provided in Reference A-1. The suggested method is described by the following equations:

$$\alpha \approx \frac{0.002}{e_y} \qquad (2)$$

$$n = \frac{\ell n\left[\frac{1}{\alpha}\left(\frac{\ell n(1+e_u)}{\ell n(1+e_y)}\right) - \frac{S_u(1+e_u)}{S_y(1+e_y)}\right]}{\ell n\left[\frac{S_u(1+e_u)}{S_y(1+e_y)}\right]} \qquad (3)$$

where S_u and S_y represent ultimate stress and yield stress respectively. They can be obtained from the ASME Code [A-2] for a wide range of temperatures. The yield strain (e_y) is determined as:

$$e_y = \frac{S_y}{E} \qquad (4)$$

where E (modulus of elasticity) can also be obtained from the ASME Code. The ultimate strain (e_u) is not specified at all temperatures in the ASME Code, hence the room temperature elongation value specified in the ASME Code, Section II [A-2] is assumed for all temperatures. The methodology in any case is not sensitive to the choice of e_u [A-1] when determining É and n by using equation (2) and (3).

It is obvious that α is a function of e_y, n is a function of α, e_u, e_y, S_u, and S_y , and both are the function of temperature. Therefore, an adjustment scheme can be used as follows where the material properties at 650°F are adjusted based on the ratio of predicted properties from Equations (2) and (3) using Code minimum properties:

$$(\alpha)_{650°F} = (\alpha)_{\text{Base, }550°F} \text{X} \frac{\text{Equation}(2)_{550°F,\ \text{Code min.property}}}{\text{Equation}(2)_{650°F,\ \text{Code min.property}}} \qquad (5)$$

$$(n)_{650°F} = (n)_{\text{Base, }550°F} \text{X} \frac{\text{Equation}(3)_{550°F,\ \text{Code min.property}}}{\text{Equation}(3)_{650°F,\ \text{Code min.property}}} \qquad (6)$$

Hence, Equations (2), (3), (4), (5) and (6) can be used to obtain R-O parameters at 650°F from the given values at 550°F.

A.3 RESULTS

The inputs into the evaluation consist of the R-O parameters provided in Tables 4-1 in the main body of the report and ASME Code properties at 550°F and 650°F. The input and results of the analysis which determines the R-O parameters at 650°F are provided in Table A-1.

A.4 REFERENCES

A-1. Cofie, N.G., Miessi, G.A., and Deardorff, A.F., "Stress-Strain Parameters in Elastic-Plastic Fracture Mechanics," Smirt 10 International Conference, August 14-18, 1989.

A-2 ASME Boiler and Pressure Vessel Code, Sections II and III Appendices, 1989 Edition.

Table A-1

Determination of Ramberg-Osgood Parameters for SMAW at 650°F

	α, 550°F	9
	n, 550°F	9.8
Temperature (°F)	550	650
E (ksi)	25550	25050
S_y (ksi)	19.35	18.5
S_u (ksi)	67	67
e_u (in/in)	0.3	0.3
e_y (in/in)	0.0007573	0.0007385
$\varepsilon_o = \ell n (1+e_y)$	0.0007571	0.0007383
$\varepsilon_u = \ell n (1+e_u)$	0.2623643	0.2623643
α'	2.6408269	2.7081081
n'	3.2348215	3.1407678
α	9.0	9.227
n	9.8	9.515